EPRI | ELECTRIC POWER RESEARCH INSTITUTE

Simulated Boiler Corrosion Studies Using Electrochemical Techniques

Technical Report

Simulated Boiler Corrosion Studies Using Electrochemical Techniques

1010187

Final Report, March 2006

EPRI Project Manager
R. B. Dooley

ELECTRIC POWER RESEARCH INSTITUTE
3420 Hillview Avenue, Palo Alto, California 94304-1395 ▪ PO Box 10412, Palo Alto, California 94303-0813 ▪ USA
800.313.3774 ▪ 650.855.2121 ▪ askepri@epri.com ▪ www.epri.com

DISCLAIMER OF WARRANTIES AND LIMITATION OF LIABILITIES

THIS DOCUMENT WAS PREPARED BY THE ORGANIZATION(S) NAMED BELOW AS AN ACCOUNT OF WORK SPONSORED OR COSPONSORED BY THE ELECTRIC POWER RESEARCH INSTITUTE, INC. (EPRI). NEITHER EPRI, ANY MEMBER OF EPRI, ANY COSPONSOR, THE ORGANIZATION(S) BELOW, NOR ANY PERSON ACTING ON BEHALF OF ANY OF THEM:

(A) MAKES ANY WARRANTY OR REPRESENTATION WHATSOEVER, EXPRESS OR IMPLIED, (I) WITH RESPECT TO THE USE OF ANY INFORMATION, APPARATUS, METHOD, PROCESS, OR SIMILAR ITEM DISCLOSED IN THIS DOCUMENT, INCLUDING MERCHANTABILITY AND FITNESS FOR A PARTICULAR PURPOSE, OR (II) THAT SUCH USE DOES NOT INFRINGE ON OR INTERFERE WITH PRIVATELY OWNED RIGHTS, INCLUDING ANY PARTY'S INTELLECTUAL PROPERTY, OR (III) THAT THIS DOCUMENT IS SUITABLE TO ANY PARTICULAR USER'S CIRCUMSTANCE; OR

(B) ASSUMES RESPONSIBILITY FOR ANY DAMAGES OR OTHER LIABILITY WHATSOEVER (INCLUDING ANY CONSEQUENTIAL DAMAGES, EVEN IF EPRI OR ANY EPRI REPRESENTATIVE HAS BEEN ADVISED OF THE POSSIBILITY OF SUCH DAMAGES) RESULTING FROM YOUR SELECTION OR USE OF THIS DOCUMENT OR ANY INFORMATION, APPARATUS, METHOD, PROCESS, OR SIMILAR ITEM DISCLOSED IN THIS DOCUMENT.

ORGANIZATION(S) THAT PREPARED THIS DOCUMENT

The Pennsylvania State University

NOTE

For further information about EPRI, call the EPRI Customer Assistance Center at 800.313.3774 or e-mail askepri@epri.com.

CITATIONS

This report was prepared by

The Pennsylvania State University
University Park, PA 16802

Principal Investigator
S. Lvov
The Energy Institute & Department of Energy and Geo-Environmental Engineering

Authors
M. Fedkin
V. Balashov
The Energy Institute

This report describes research sponsored by the Electric Power Research Institute (EPRI).

The report is a corporate document that should be cited in the literature in the following manner:

Simulated Boiler Corrosion Studies Using Electrochemical Techniques. EPRI, Palo Alto, CA: 2006. 1010187.

PRODUCT DESCRIPTION

Boiler waterside corrosion in fossil plants represents a serious cause of availability and performance loss. EPRI cycle chemistry guidelines provide control curves based on cation conductivity. This report provides the first results of an electrochemistry study to derive new control curves for each cycle chemistry treatment that are based on corrosion.

Results and Findings

The measuring tools for corrosion studies at temperatures up to 360°C (680°F) and pressures up to 26 MPa (3770 psi) were developed and tested. These include a flow-through hydrothermal cell, an annular duct flow-through electrode assembly, and an Ag/AgCl reference electrode. The first DC polarization and electrochemical impedance spectroscopy (EIS) measurements were made in dilute electrolyte solutions. Initial corrosion rates for carbon steel were determined for all-volatile treatment (AVT).

Challenges and Objective

The overall work represents a major new approach to understanding and controlling fossil plant boiler corrosion. Almost no electrochemical studies have been conducted in high temperature aqueous environments at temperatures and pressures representative of boiler operating conditions. The objective of this initial study was to develop the electrochemical tools to measure corrosion in the aqueous solutions corresponding to the main fossil chemical treatments, that is, all-volatile treatment (AVT), phosphate continuum (PC), caustic treatment (CT), and oxygenated treatment (OT).

Applications, Value, and Use

Once the equipment has been designed and operated, it will be able to produce comparative boiler corrosion control curves. These curves will then be incorporated into the EPRI guidelines and used by fossil plants worldwide.

EPRI Perspective

EPRI has recently published three fossil plant treatment guidelines for AVT (1004187), PC/CT (1004188), and OT (1004925). These are key to the overall availability of fossil plants but currently use indirect measurements of corrosion in the cycle. The main parameter is cation conductivity. This current research, together with the research on deposition, will eventually lead to an approach using direct indicators of corrosion processes in the boiler.

Approach

The project team decided to use a combined approach of *in situ* and *ex situ* experimental methods for determining the corrosion rates. They incorporated two electrochemical methods within the autoclave assembly—DC polarization and EIS. They also designed the *ex situ* technique, which involves mass loss of a similar steel specimen. The team commissioned the apparatus and conducted a number of initial tests up to 360°C (680°F) in simulated AVT solution with chloride and sulfate additions.

Keywords

Power plant availability
Boilers
Boiler water chemistry
Corrosion
Electrochemistry

ABSTRACT

This report describes the progress in the electrochemical corrosion measurements of carbon steel under fossil plant boiler water treatment regimes. At this stage in the research, the experimental tools for high temperature corrosion measurements have been successfully developed. The first experimental data on corrosion rates for all-volatile treatment (AVT) up to 360°C (680°F) and at 18 MPa (2610 psi) have been measured. Two electrochemical methods have been used in parallel: DC polarization and electrochemical impedance spectroscopy (EIS). The results from these two methods are compared with conventional mass loss data.

CONTENTS

LIST OF FIGURES

LIST OF TABLES

1
INTRODUCTION

This research project, which started on April 1st of 2005, involves electrochemical corrosion studies of carbon steel (SA210A1) under the conditions of several chemical treatment regimes: (1) All-volatile Treatment (AVT), (2) Phosphate Continuum (PC), (3) Caustic Treatment (CV), and (4) Oxygenated Treatment (OT). Each of these regimes provides a certain chemical environment and is used according to the presently existing EPRI cycle chemistry guidelines. The long-term goal of the study is to determine the maximum permissible levels of various ionic species in the boiler water and to provide scientifically justified guidelines for corrosion protection up to 350°C (662°F). This work is being conducted at The Energy Institute Electrochemical Laboratory of The Pennsylvania State University. A unique feature of the approach is the use of a number of electrochemical techniques specifically designed for high temperature corrosion studies under high temperature subcritical and supercritical solutions.

The electrochemical measurements at temperatures above 300°C (572°F) present a specific challenge due to limitations on material stability in the near-critical hydrothermal environments. This temperature boundary is the upper stability limit of Teflon®, above which no inert and isolating polymeric material is available for use in the design of high temperature electrochemical systems. Almost no studies have been performed to experimentally measure the corrosion current in high temperature aqueous environments at temperatures above 300°C. Based on available literature reviews [1–5], the methodology for studying high temperature electrochemical kinetics and corrosion processes remains “under construction” and some serious experimental issues in this area, such as proper control of the mass transport processes, are yet to be resolved.

The scope of the electrochemical corrosion studies defined for this project involves the following tasks:

- Task 1. Design of measuring tools, cycle water preparation, and equipment commissioning leading to initial runs.
- Task 2. Determination of optimum chemistry and bounding limits for AVT.
- Task 3. Determination of optimum chemistry and bounding limits for OT.
- Task 4. Determination of optimum chemistry and bounding limits for PC.
- Task 5. Determination of optimum chemistry and bounding limits for CT and OT.
- Task 6. Report findings in the form of control charts and tables suitable for incorporation in EPRI Guidelines.

The work during the nine-month project of 2005 was particularly focused on Task 1 and the beginning of Task 2. Systematic coverage of Tasks 2–6 is planned as the next step in the future studies. The accomplished research to date has involved designing, constructing, and testing the high temperature electrodes, electrode assemblies, and associated measuring tools for the high temperature corrosion studies up to 360°C (680°F) and 3770 psi (26 MPa). It was also very important to prove the possibility of using these tools for obtaining the corrosion rates for carbon steel in very dilute electrolyte solutions, such as AVT, over the range of targeted temperature/pressure parameters. The experimental electrochemical measurements were performed using a flow-through electrochemical apparatus, which allowed all the measurements to be performed under steady-state conditions in a well-characterized hydrodynamic environment. Two electrochemical techniques were used in parallel to determine the corrosion rates—DC polarization and electrochemical impedance spectroscopy (EIS). The electrochemical data were correlated with the mass loss analysis. In the future, the applicability of using electrochemical noise analysis (ENA) for corrosion studies in dilute solutions of interest will be verified.

2
BACKGROUND

2.1 Theoretical Principles of Electrochemical Corrosion

Most electrochemical processes are heterogeneous by nature and involve both mass transport and electron transfer processes [6]. Electrochemical reactions involve charged species, and the rate of an electron transfer reaction depends on the electric potential difference between the phases (e.g., between the electrode surface and the solution). The mass transport processes mainly include diffusion, conduction, and convection, which should be taken into account if the electron transfer reaction parameters are to be derived from the experimental measurements.

A specific feature of the electrochemical approach is that the total rate of the electrochemical process can be determined by measuring the current density, *j*, in an external electrical circuit [6]. The reaction rate, *v* (per unit surface area), is related to the current density as follows:

$$j = nFv \qquad \textbf{Equation 2-1}$$

where *n* is the number of electrons involved in the electrochemical reaction. Assuming a reduction/oxidation (redox) electrode reaction as a first-order interfacial process,

$$O + ne^- \underset{k_O}{\overset{k_R}{\leftrightarrow}} R \qquad \textbf{Equation 2-2}$$

the reaction rate will be defined by (i) the heterogeneous rate constants for the reduction, k_R, and oxidation, k_0, processes; and (ii) the activities of *O*, $a_O^{\#}$, and *R*, $a_R^{\#}$, at the electrode surface as follows:

$$v = k_O a_R^{\#} - k_R a_O^{\#} \qquad \textbf{Equation 2-3}$$

Within the framework of the activation complex theory [6, 7] the current density provided by the redox reaction (Equation 2-2) can be expressed through the Butler-Volmer equation:

$$j = nFk_0 \left(a_R^{\#} \exp\left(\frac{\alpha nF(E - E_{00})}{RT}\right) - a_O^{\#} \exp\left(\frac{-(1-\alpha)nF(E - E_{00})}{RT}\right)\right) \qquad \textbf{Equation 2-4}$$

where E_{00} is the standard equilibrium potential of Equation 2-2, α and (1-α) are the transfer coefficients of the oxidation and reduction reactions, respectively. Using the Nernst equation

Background

$$E_0 = E_{00} + \frac{RT}{nF} \ln \frac{a_O^{\#}}{a_R^{\#}}$$ **Equation 2-5**

for the equilibrium potential, E_0, and the overpotential $\eta = E - E_0$, which is the deviation from equilibrium potential, the Butler-Volmer equation can be re-written as follows:

$$j = j_0 \left(\exp\left(\frac{\alpha nF\eta}{RT}\right) - \exp\left(\frac{-(1-\alpha)nF\eta}{RT}\right)\right)$$ **Equation 2-6**

where j_0 is the exchange current density. At the equilibrium potential E_0, the anodic and cathodic currents have the opposite signs and the same magnitude of j_0, and thus cancel out. Combining Equations 2-4 and 2-5, it can be shown that j_0 is mainly defined by the rate constant, k_0, and also depends on the activities of *O* and *R* as follows:

$$j_0 = nFk_0 (a_R^{\#})^{1-\alpha} (a_O^{\#})^{\alpha}$$ **Equation 2-7**

In the general case of an electrochemical corrosion process, metal degrades through an anodic reaction, and a cathodic reaction should simultaneously occur at the same surface. For example, in the case of iron corrosion in a de-oxygenated aqueous solution, iron would electrochemically oxidize via the following anodic process:

$$Fe \xrightarrow{k_a} Fe^{2+} + 2e$$ **Equation 2-8**

and hydrogen reduction can occur as a cathodic process:

$$2H^+ + 2e^- \xrightarrow{k_c} H_2$$ **Equation 2-9**

If $nF|\eta| >> RT$, Equation 2-6 can be written for the anodic half-reaction of corrosion (Equation 2-8) as:

$$j_a = j_{0,a} \exp\frac{\alpha_a nF(E - E_{0,a})}{RT}$$ **Equation 2-10**

and for the cathodic half-reaction (Equation 2-9) as:

$$j_c = -j_{0,c} \exp -\frac{\alpha_c nF(E - E_{0,c})}{RT}$$ **Equation 2-11**

Using Equations 2-10 and 2-11 for the coupled anodic and cathodic half-reactions (Equations 2-8 and 2-9), an equation can be developed which relates the measured current density, *j*, to the measured electric potential, *E*:

$$j = j_a + j_c = j_{corr}\left(\exp\left(\frac{\alpha_a nF(E - E_{corr})}{RT}\right) - \exp\left(\frac{-\alpha_c nF(E - E_{corr})}{RT}\right)\right) \quad \textbf{Equation 2-12}$$

where j_c and j_a are, respectively, the cathodic and anodic current densities, α_c and α_a are, respectively, the cathodic and anodic transfer coefficients, j_{corr} is the corrosion current, and E_{corr} is the corrosion potential. Note that in Equation 2-12, $\alpha_c \neq \alpha_a$, and there is no reason why $\alpha_c + \alpha_a = 1$. Also, it should be mentioned that E_{corr} is a measurable value as an open circuit potential, while j_{corr} cannot be directly measured. However, a number of techniques [6] are used to calculate j_{corr} and these electrochemical methods are addressed in the following section.

It is important that the electrode surface is actually divided into local anodic and cathodic cells [6]. The spatial distribution of the cathodic and anodic regions is due to local irregularities in the electrode microstructure, grain boundaries, inclusions, etc. If the anodic reaction obeys the Tafel law on the fraction of surface area θ_a and the cathodic reaction obeys the Tafel law on the fraction of surface area θ_c, the corrosion current density can be expressed as follows:

$$j_{corr} = j_{0,a}\theta_a = j_{0,c}\theta_c \quad \textbf{Equation 2-13}$$

where $j_{0,a}$ and $j_{0,c}$ are the mean current densities on the anodic and cathodic area fractions, respectively, at the corrosion potential. The substitution of Equation 2-13 into Equation 2-12 and the following differentiation leads to the following expression for the polarization resistance:

$$\frac{1}{R_p} = \frac{dj}{dE} = j_{corr}(\alpha_a + \alpha_c)\frac{nF}{RT} + j_{0,a}\frac{d\theta_a}{dE} - j_{o,c}\frac{d\theta_c}{dE} \quad \textbf{Equation 2-14}$$

which confirms that the Stern-Geary equation for the polarization resistance is valid only if the fractional surface areas are independent of the potential around E_{corr}. On the other hand, the charge transfer resistance R_{CT} fulfills the Stern-Geary equation in the case when the electrode surface is divided into numerous local anodic and cathodic cells with potential-dependent fractional areas:

$$\frac{1}{R_{CT}} = j_{corr}(\alpha_a + \alpha_c)\frac{nF}{RT} \quad \textbf{Equation 2-15}$$

Therefore, electrochemical impedance spectroscopy (EIS) allows the terms $d\theta_a/dE$ and $d\theta_c/dE$ to be separated from dj/dE and, therefore, R_{CT} can be determined.

Background

The change in θ with E implies variations in species surface coverage (for example, adsorption/desorption processes) and, therefore, requires a certain time to occur. For simple systems, these changes follow an exponent-type function with a time constant (τ) that conveys information about the kinetics of the process. In a simple case, with a single parameter representing the surface coverage (θ) of an intermediate species, the Faradaic impedance can be expressed by the equation:

$$\frac{1}{Z_F} = \frac{dj}{dE} = \frac{1}{R_{CT}} + \frac{\partial j}{\partial E}\Big|_E \frac{d\theta}{dE} = \frac{1}{R_{CT}} + j_0 \frac{C}{1 + i\omega\tau}, \qquad \textbf{Equation 2-16}$$

where Z_F is the Faradaic impedance, $\omega = 2\pi f$ is the angle (in radian) frequency, f is the frequency in Hz, and C is a constant. According to Equation 2-16, at high frequencies, the Faradaic impedance is defined by the charge transfer resistance (R_{CT}).

2.2 Experimental Principles of Electrochemical Corrosion Studies

2.2.1 Electrodes

Two-electrode and three-electrode schemes are most typical in electrochemical measurements of corrosion parameters. Either scheme is chosen based on a specific goal. If only two electrodes are used in corrosion studies, both of them are not in equilibrium, and, consequently, there is an overpotential, η, on each of the electrodes. The potential difference measured between the two electrodes is determined by the two overpotentials, hence it is not convenient to determine the actual potential of the corroding (working) electrode. Therefore, to obtain the potential value more precisely, a third (counter) electrode must be used. In the three-electrode scheme, current flows between the working and the counter electrodes, and a high impedance voltmeter is used to measure the potential difference between the working and reference electrodes. In this case, the reference electrode shows a negligible overpotential and remains very close to its equilibrium value. Using the three-electrode method, the working electrode potential and its changes under electric current flow can be properly measured with respect to a reference potential, which should not change over the experimental time.

It is not very important what kind of material is used for the counter electrode, but one should make sure that possible electrochemical degradation of the counter electrode does not contaminate the test solution. Also, the surface of the counter electrode should be sufficiently large (e.g. Pt coil, foil, or mesh) to avoid a high current density at the counter electrode.

A reference electrode for high temperature corrosion studies must have a stable and reproducible potential independent of changes in the test solution at the working electrode. Also, it is highly desirable that the standard potential of the reference electrode is thermodynamically defined with respect to the standard hydrogen electrode (SHE) scale. If the reference electrode solution is bridged into the test solution, the diffusion (junction) potential between the test and reference solutions should be taken into account. To date, two types of reference electrodes have been used for high temperature corrosion studies: (i) internal reference electrode operating in the high

temperature environment and (ii) external reference electrode working at the room temperature, but connected to the high temperature environment by a non-isothermal electrolyte bridge. Use of previously tested electrochemical couples (e.g., Ag/AgCl, Ag/AgBr, Hg/Hg_2Cl_2, Hg/Hg_2SO_4, Ag/Ag_2SO_4, Hg/HgO, and $Pb/PbSO_4$) as an internal high temperature reference electrode is problematic at temperatures above 250°C (482°F) because of chemical degradation in harsh hydrothermal environments. In an external (pressure-balanced) reference electrode, an electrochemical couple (e.g., Ag/AgCl) is kept at the ambient temperature, and the electrode compartment is connected to the high temperature zone by a non-isothermal electrolyte bridge. One of the latest designs of the external reference electrode employs the flow-through principle, which minimizes interference from contaminates (e.g., corrosion products) and from the Soret effect. In this case, however, an additional complication can be caused by the streaming potential generated by the electrolyte solution flow through a thin capillary channel. This potential should also be taken into account. The flow-through external reference electrode can be used at any desirable temperature and pressure (until the aqueous solution is sufficiently conductive), which was experimentally confirmed up to 400°C (752°F) and 35 MPa (5075 psi) [8, 9]. Since the reference solution flows through the electrode at a constant velocity, the concentration of the solution across the electrolyte bridge remains constant, and any uncertainty in the thermal diffusion potential can be eliminated at a given temperature and pressure. Using 0.1 mol kg^{-1} NaCl aqueous solution commonly employed in the non-isothermal electrolyte bridge, the potential of the flow-through external reference electrode was found to be stable within 1–3 mV.

2.2.2 IR Drop

When current, *I*, passes through an electrolyte, an ohmic resistance, *R*, is observed between the electrodes inserted into the electrolyte. The *IR* drop is an ohmic voltage that originates from the electric current flowing in ionic solutions. The *IR* drop is often an unknown value and should be either eliminated or minimized. Different approaches can be used to solve the *IR* drop problem [6]. One of the approaches is to use the Luggin capillary, which is a thin tube made out of glass or Teflon for temperatures below 250°C (482°F) and out of ceramics for temperatures above 250°C (482°F). The tip of the Luggin capillary is placed as close as possible to the working electrode surface, while its other end is connected to an electrochemical couple of the reference electrode. If the Luggin capillary is filled with a highly conductive electrolyte, the *IR* drop is significantly decreased. Also, if a high-impedance voltmeter is used to prevent undesirable current flow through the Luggin capillary, the absence of current eliminates the *IR* drop. In electrochemical kinetics and corrosion studies, some current is necessary, and the *IR* drop cannot be completely avoided. In this case, *IR* drop should be minimized and can be estimated using, for example, the current interruption technique.

2.2.3 Hydrodynamic Control

The experimental j_{corr} data at temperatures in the temperature range between 100 and 300°C (212 and 572°F) sometimes are not credible, because the experimental measurements were carried out without any control of the transport processes. For instance, experimental data obtained using an autoclave technique reflect both the mass transport and charge transfer phenomena. However, the above-mentioned parameters (j_o, α) in an electrochemical kinetics

experiment and (j_{corr}, α_a, α_c) in a corrosion study are strictly confined to charge transfer, and it is necessary to delineate these phenomena in any electrochemical kinetics (corrosion) experiment. To solve this problem, one needs to carry out the electrochemical measurements under well-defined hydrodynamic conditions. The traditional rotating-disk (ring) electrode system is normally used for this purpose at ambient temperature, but there is no design implementing the rotating-disk method under hydrothermal conditions. Thus far, only a few controlled hydrodynamic systems for electrochemical kinetics (corrosion) studies have been tested at temperatures below 300°C (572°F) (where Teflon is still mechanically stable): a wall-tube electrode cell [10] (tested up to 200°C, 392°F) and tubular flow-through electrochemical system [11, 12] (up to 250°C, 482°). Both approaches can be promising for high temperature subcritical and supercritical aqueous conditions.

2.2.4 Electrochemical Techniques

Thus far, only a few credible corrosion studies have been carried out at temperatures above 300°C (572°F). References [13] and [14] report studies in which the steady-state cyclic voltammetry was applied to learn a number of electrochemical reactions in near-critical and supercritical fluids at temperatures up to 385°C (725°F). The authors of Reference [15] applied the electrochemical impedance spectroscopy for studying nickel alloy 600 at temperatures up to 350°C (662°F) in lithiated water containing hydrogen. Electrochemical noise sensors have also been shown to be capable of measuring the electrochemical kinetics and corrosion rates in flowing subcritical and supercritical fluids at temperatures ranging from 150 to 390°C (392 to 734°F), and pressure of 25 MPa (3625 psi) [16]. Based on these studies, the rate of the general electrochemical corrosion of a stainless steel was estimated. Although the electrochemical noise analysis has yet to be rendered quantitative, the results obtained thus far [16] suggest that this method could be an effective tool for studying the electrochemical kinetics phenomena in high temperature subcritical and supercritical aqueous solutions.

In this study, the following electrochemical methods are considered the most beneficial for high temperature corrosion rate measurements: (1) DC polarization, (2) electrochemical impedance spectroscopy (EIS), and (3) electrochemical noise (EN). The principles of these techniques are briefly described below.

DC Polarization. If in a corrosion process, the anodic and cathodic half-reactions compensate for each other, no net electron transfer is observed, and the corrosion current (I_{corr}) cannot be directly measured. However, the electrode potential, E_{corr}, corresponding to I_{corr} can be measured using the above-described three-electrode configuration. Moreover, if the electrode potential is forcefully shifted from the E_{corr}, the response of the system will be an electrical current, which can be experimentally measured [17]. At sufficient deviations of the applied potential from the E_{corr}, either anodic or cathodic current dominates and the classic Tafel analysis can be used to fit the experimental data [17, 18]. The I_{corr} value for a particular electrochemical system is derived at the intersection of linearly extrapolated anodic and cathodic current curves, which fit experimental data at potentials significantly higher and lower than E_{corr}.

Electrochemical Impedance Spectroscopy (EIS). The electrochemical impedance is measured by applying a small perturbation signal (AC potential) to an electrochemical cell and measuring the response of the system (current through the cell). The "small signal" implies that the perturbation of the system is so low that the response is linear, i.e., harmonic generation and frequency mix products can be neglected [19]. The EIS data presented as Nyquist diagrams (imaginary impedance plotted vs. real impedance) are analyzed by the equivalent electrical circuit (EEC) model fitting. The EEC consists of resistors, capacitors, and inductors in serial and parallel combinations, which are chosen based on the best fit of the model and measured impedance. The model of EEC is constrained by the physical design of the electrochemical cell.

Electrochemical Noise (EN). This method deals with random fluctuations in current and potential around their open circuit values that are often observed in electrochemical systems [20–30]. In this approach, two identical electrodes made out of a metal of interest are used, and a dynamic platinum electrode is used as a reference electrode. Based on the simultaneous monitoring of the electrode potential and coupling current from two identical electrodes, the noise resistance (R_n) can be determined as a ratio of the standard deviations of the potential noise (σ_E) and coupled current noise (σ_I). As was previously suggested [21], R_n is related to the polarization resistance (R_p), which is commonly determined by the linear polarization techniques. A few attempts have been made to use the EN techniques for corrosion studies at elevated temperatures [16, 32–34]. In one study [16], a hydrothermal cell was used with a flow-through EN-sensor to measure the electrochemical noise in very dilute solutions. A steady correlation was established between the reciprocal R_n and the corrosion rates of Type 304 SS steel obtained from conventional mass loss measurements in the temperature range of 150–390°C (302–734°F). These data confirm the high potential of using the EN techniques for corrosion studies in high temperature aqueous solutions, but the techniques should be further checked on how exactly the polarization resistance is related to the corrosion current.

3
EXPERIMENTAL TECHNIQUES

3.1 Electrochemical Cell and Design of Electrodes

The high temperature corrosion studies have been conducted in a high temperature flow-through electrochemical cell [9, 35, 36] (Figure 3-1). The cell was previously proved to be highly reliable for potentiometric studies of dilute electrolyte solutions over a wide range of temperatures (up to 400°C, 752°F) [2].

The cell body is made of a highly corrosion-resistant alloy, Hastelloy-B, and is designed for reliable operation at temperatures up to 400°C (752°F). The electrochemical cell has four ports for installation of the high temperature electrodes and inlets and outlets of test solution. The schematic of the port configuration is shown in Figure 3-2.

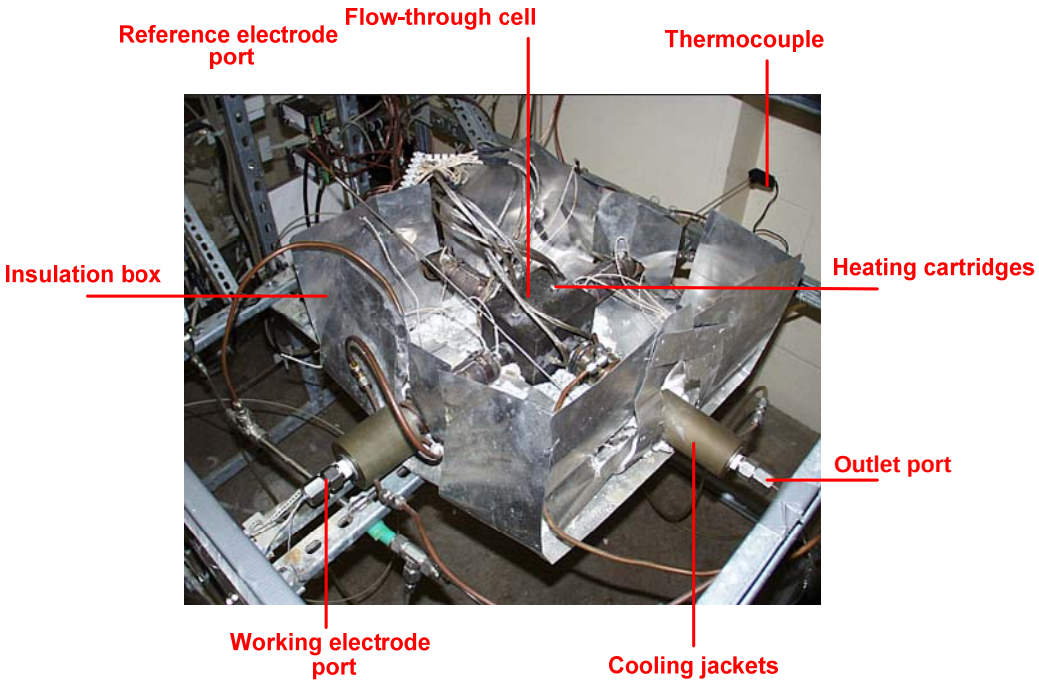

Figure 3-1
View of the High Temperature Flow-Through Electrochemical Cell with Installed Electrodes and Heaters

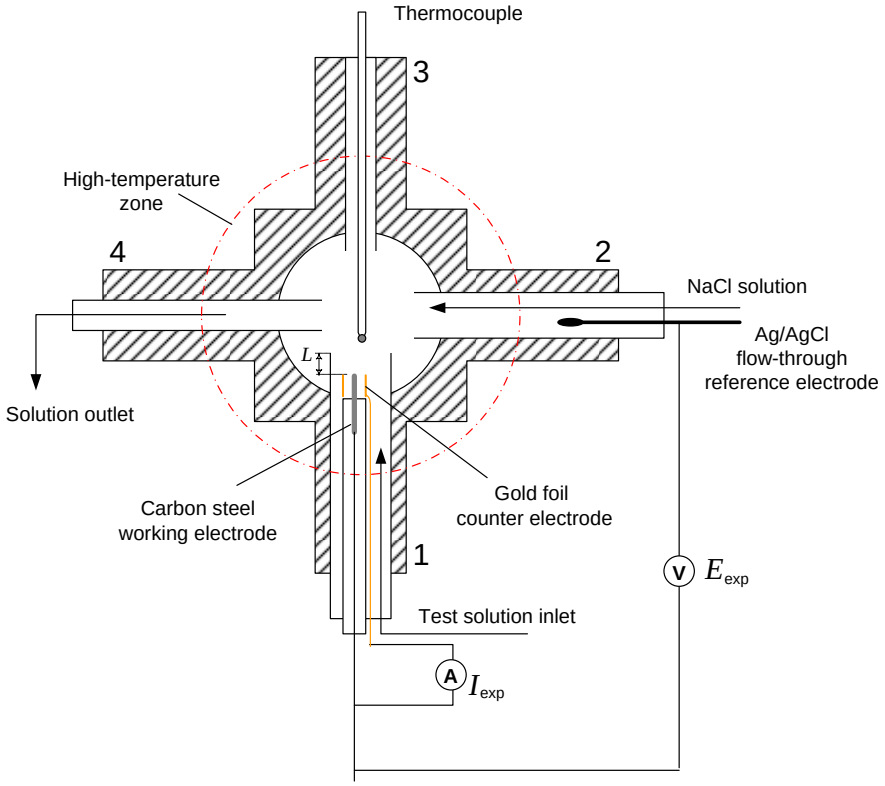

Figure 3-2
Configuration of the High Temperature Flow-Through Electrochemical Cell. Ports: 1 – Working/Counter Electrode Assembly and Test Solution Inlet, 2 – External Ag/AgCl Reference Electrode, 3 – Thermocouple, and 4 – Solution Outlet.

Operation of the cell is facilitated by the following equipment. High pressure chromatography pumps (HPCP, Acuflow Series II) with all metal-free parts are used to supply the test solution to the working electrode port and reference solution to the reference electrode port. A spring pressure-relief valve controls the outlet pressure. Two pressure gauges are used to monitor pressure at the inlet and outlet of the cell in the cold zone. Eight cartridge heaters inserted into the cell body provide the main heating, and additional pre-heaters are installed on the cell inlet/oulet tubes (arms) to minimize temperature gradients. Omega temperature controllers are used to control temperature. A controlling thermocouple for the pre-heaters is installed close to the main heater and touches the metal outside of the cell. A measuring and controlling thermocouple for the main heater is installed in Port 3 inside the cell and contacts the experimental solution in the close vicinity of the working electrode. The four inlet/outlet tubes of the cell have cooling jackets on their rear ends, which protect the Teflon fittings in the sealing glands. Cold tap water is supplied continuously through the cooling jackets during a high temperature experiment. The Gamry Electrochemical Measurements system is used to perform electrochemical measurements. The view of the experimental system setup is shown in Figure 3-3. The experimental solution was supplied to the flow-through cell from the solution preparation station, which is described in detail in the following sections.

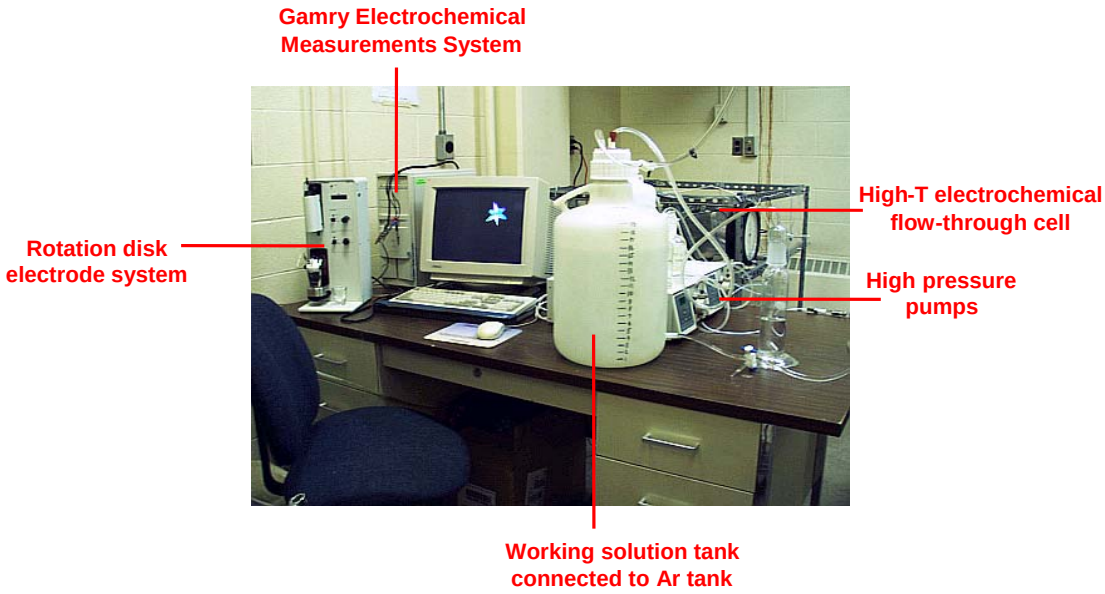

Figure 3-3
View of the Experimental System for High Temperature Electrochemical Corrosion Measurements

Initial operational tests of the high temperature electrochemical cell showed that in the flow-through regime, the temperature in the working zone of the cell remained stable with the maximum variation of ±1° up to 350°C (662°F). Pressure was found to be stable within the target parameter range.

3.2 Flow-Through Working and Counter Electrodes

One of the first important steps in configuring the high temperature electrochemical cell for corrosion studies was to determine the most efficient electrode geometry, which would provide measurable corrosion current values. Both theoretical calculations and preliminary experimental measurements were necessary to accomplish this task. For comparison, the limiting current was calculated for two geometrical types of electrochemical cell with controlled hydrodynamics: (1) annulus duct and (2) wall-tube. In the first case, the solution flow occurs between the cylindrical surfaces of the working and counter electrodes [37]. In the second case, the solution jet is directed onto the flat surface of the working electrode [10, 37]. Calculations showed that in both cases the electric current values fall within the range 10^{-6} – 10^{-4} A cm^{-2}, which allows use of the DC polarization method in the framework of the DC105 Corrosion Measurement System [17]. Based on the analysis, it was decided that the annulus duct geometry is a preferable technique for the high temperature cell configuration due to a somewhat higher magnitude of the limiting current compared to the wall-tube geometry and a simpler experimental design of the electrode assembly.

In the annular duct geometry, the test solution flows through a ring-section channel between the outer cylindrical surface of the rod-shaped working electrode and the inner cylindrical surface of the tubular counter electrode (Figure 3-4).

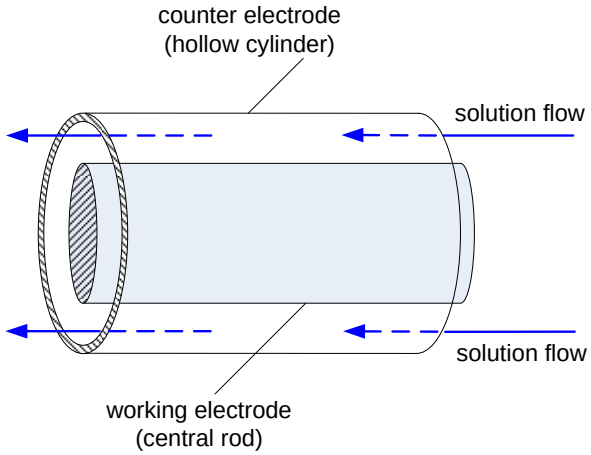

Figure 3-4
Annular Duct Geometry Adopted for the Flow-Through Working/Counter Electrode Assembly for the High Temperature Corrosion Studies

For the annular duct configuration, the electrical current density in the mass transfer limit can be described by the following equation [37]:

$$j = 2FC^{0}_{Fe++}k^{0}_{m,ad}(D_{Fe++})^{2/3} \quad , \qquad \textbf{Equation 3-1}$$

where F is the Faraday constant, C^{0}_{Fe++} is the concentration of Fe^{++} ions at the surface of the working electrode, $k^{0}_{m,ad}$ is the mass transfer coefficient, and D_{Fe++} is the diffusion coefficient of Fe^{++} ion in an aqueous solution. In the case of the annular duct electrode geometry,

$$k^{0}_{m,ad} = \alpha_{ad}\varphi(r_1/r_2)\left(\frac{u_m}{d_e}\right)^{1/3} L^{-1/3}, \qquad \textbf{Equation 3-2}$$

where u_m is the average flow velocity of the aqueous solution in the annulus duct, d_e is the width of the annulus duct $(r_2 - r_1)$, L is the effective length of the working electrode, $\varphi(r_1/r_2)$ is the function of radii ratio, and α_{ad} is a numeric coefficient (equal to 1.614).

The electric current is determined through the following equation:

$$I = 2\pi r_1 L j \quad . \qquad \textbf{Equation 3-3}$$

The average velocity of the solution flow in the duct is calculated as follows:

$$u_m = \frac{Q\rho^{n.c.}_{H2O}}{\pi(r_2^2 - r_1^2)\rho_{H2O}}, \qquad \textbf{Equation 3-4}$$

where Q is the volume flow rate of the aqueous solution under normal conditions, $\rho_{H2O}^{n.c.}$ is the water density at atmospheric pressure and room temperature, and ρ_{H2O} is the water density at the temperature and pressure of the corrosion experiment. The densities of dilute aqueous solutions can be approximated by density of pure water without any significant loss in accuracy.

At the temperatures and pressures of interest (350°C, 662°F and 18 MPa, 2610 psi), the water density is 0.548 g cm^{-3}, and the estimated value of the diffusion coefficient is 10^{-4} cm^2 s^{-1} [38]. In this calculation, the following geometrical parameters were adopted for the working electrode: the effective length, L =1 cm; the working electrode (carbon steel rod) radius, r_1=1.5 mm; the tubular counter electrode radius, r_2 =3.5 mm; and solution flow rate, Q=5 cm^3 min^{-1}.

For the Fe^{2+} concentration range 10^{-6} – 10^{-4} mol kg^{-1}, Equation 3-1 yields the electric current densities in a range of 10^{-6} to 10^{-4} A cm^{-2}, which is perfectly acceptable for using the DC polarization method. In the case of the rotation disk electrode (RDE), the limiting current is described by the same equation with the mass transfer coefficient,

$$k_{m,rd}^{0} = \alpha_{rd}(\omega')^{1/2}\nu^{-1/6}, \qquad \textbf{Equation 3-5}$$

where α_{rd} = 1.51, ω' is the rotation speed in revolutions per second, and $\nu = \eta/\rho$ is the kinematic viscosity of aqueous solution.

In this study, the above-described annular duct electrode configuration was implemented for high temperature DC polarization measurements in the design shown in Figure 3-5. This schematic demonstrates the working/counter electrode assembly, in which the carbon steel rod (sample, 3 mm OD, length 25 mm) at the center represents the working electrode, and the thin cylinder made out of gold foil (5 mm ID) serves as a counter electrode. The working and counter electrodes have respectively welded-on stainless steel and gold terminal wires connected to the electrochemical measurements system. The upper part of the carbon steel rod (working electrode) and its terminal wire are isolated with an alumina cement, so that the working electrode is exposed to the experimental solution only in the target-temperature zone. The inner ceramic tube is used as a holder for the working electrode and at the same time it works as an insulator for the terminal wire in the hot zone. The outer ceramic tube is used to hold the counter electrode and, at the same time, to provide the necessary flow channel for the experimental solution in the hot zone. At the rear (cold) end of the assembly, the outer ceramic tube is connected with a Teflon tube. Both electrode terminals and the solution inlet capillary are coated with Teflon and fitted in a high pressure Conax gland. The working/counter electrode assembly described above is shown in Figure 3-6.

In the working annular duct zone, the test solution passes between the surfaces of the working and counter electrodes, which form a channel 2 mm wide. This is the only zone where the carbon steel sample contacts the test solution.

The final parameters of the working/counter electrode assembly with the annular duct geometry were L = 1.27 cm, r_1 = 0.15 cm, and r_2 = 0.67 cm. These parameters were used to calculate the mass transfer coefficients (Equations 2-15 and 3-1) for different solution flow rates and the corresponding RDE rotation speeds at 25°C (77°F). The kinematic viscosity of water at 25°C (77°F) is 8.93 10^{-7} m^2 s^{-1}. These data are presented in Table 3-1.

Prior to high temperature measurements, the constructed working/counter electrode assembly was subject to a number of preliminary electrochemical tests. The appropriateness of this geometry for corrosion measurements was verified step by step by the DC polarization measurements, as further shown in Section 4.1.

Table 3-1
Correspondence Between the Flow Rates Through Working/Counter Electrode Assembly with Annular Duct Geometry and the Equivalent Rotation Speeds of the Rotating Disk Electrode

Q/ cm^3 min^{-1}	u_m /m s^{-1}	k_m^0 /(m s)$^{-1/3}$	Equivalent RPM
1	5.9 10^{-4}	5.74	8
5	3.0 10^{-3}	9.81	24
8	4.7 10^{-3}	11.47	32
20	1.2 10^{-2}	15.57	60

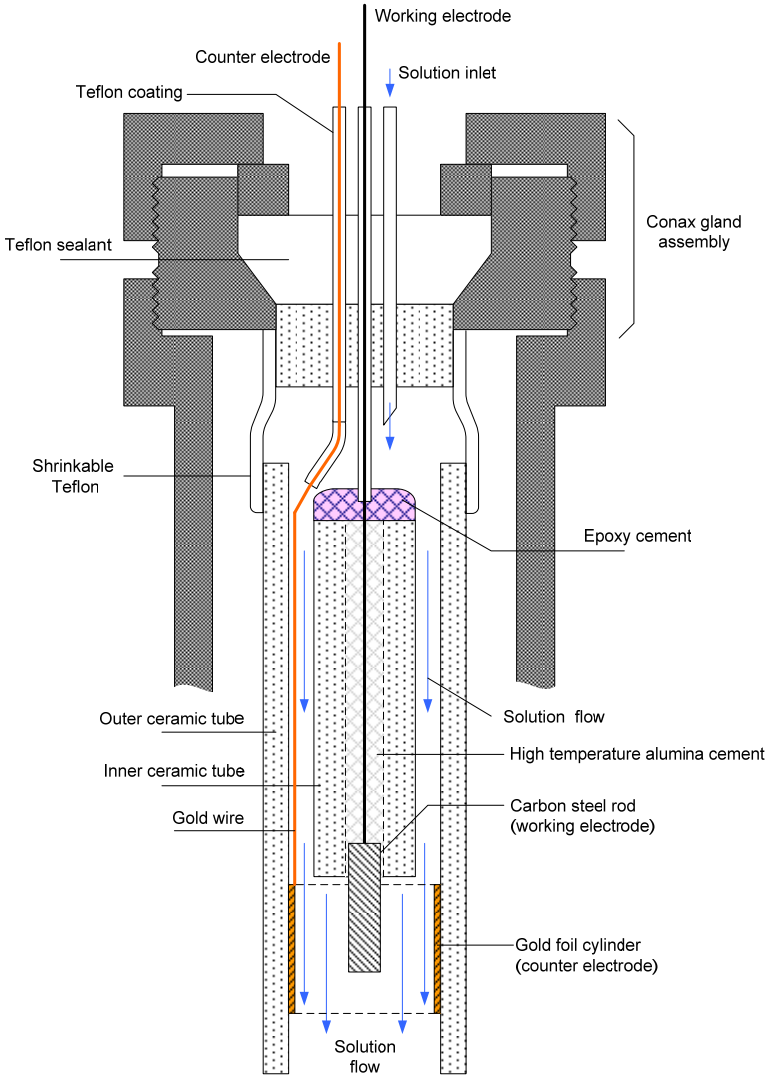

Figure 3-5
Design of the Working/Counter Electrode Assembly for High Temperature Electrochemical Corrosion Measurements

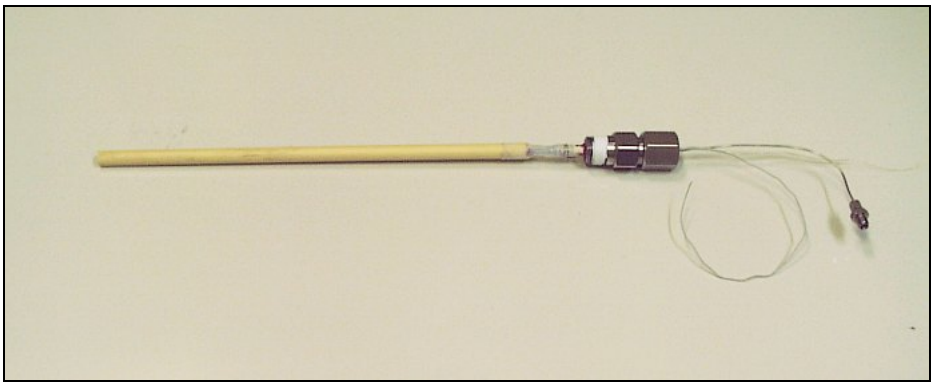

Figure 3-6
The Working/Counter Electrode Assembly

3.3 Flow-Through Ag/AgCl Reference Electrode

An external flow-through Ag/AgCl reference electrode was prepared for electrochemical corrosion studies. The schematic of the electrode design is given in Figure 3-7. According to previous studies [39], this electrode allows the potential to be measured accurate to ±3 mV at temperatures up to 400°C (752°F). The reference 0.1 mol kg^{-1} NaCl(aq) solution flows through the electrode at a constant velocity in a constant geometry. Thus, the solution concentration across the thermal liquid junction remains constant. The flow-through Ag/AgCl reference electrode was installed in Port 2 of the high temperature electrochemical cell as shown in Figure 3-2. The newly prepared Ag/AgCl flow-through reference electrode was first tested at the ambient conditions, and its potential was compared to the potential of a commercial Ag/AgCl electrode in the rotation-disk electrode system (RDE-2). The results proved to be in a good agreement.

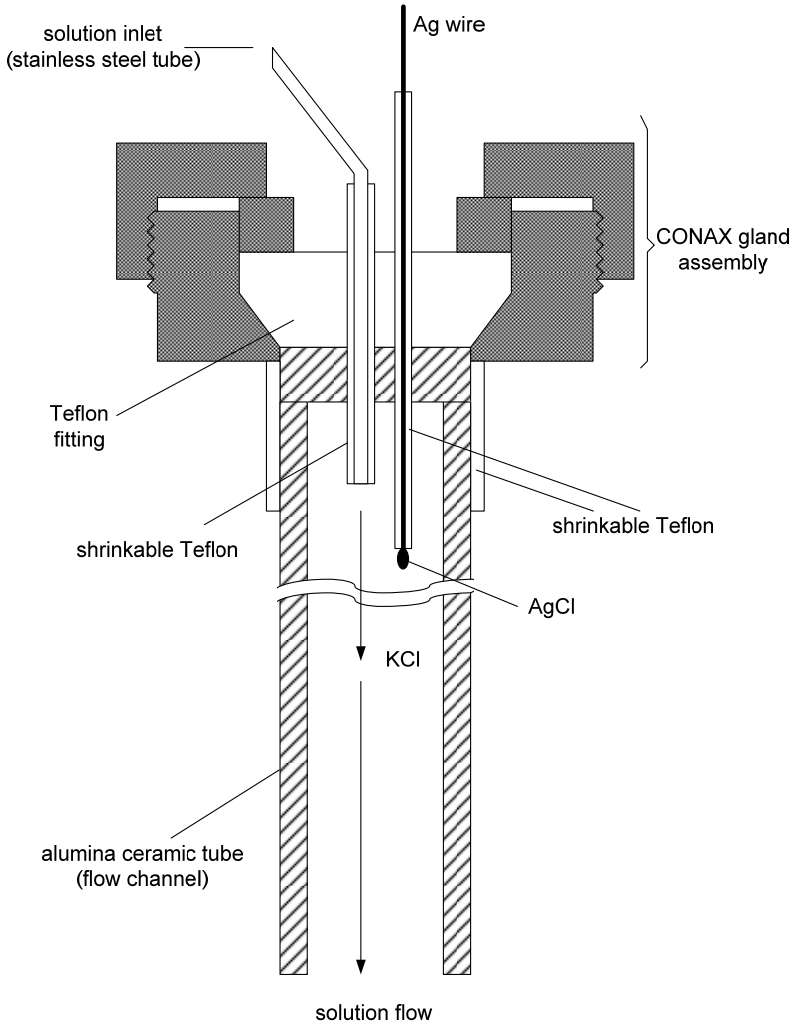

Figure 3-7
Schematic of the Flow-Through Ag/AgCl Reference Electrode

3.4 Flow-Through Electrochemical Noise Sensor

Initially, the electrochemical noise analysis (ENA) was planned as one of the primary methods to study electrochemical corrosion of carbon steel. However, in the course of the preliminary DC polarization measurements using the rotation-disk electrode (RDE-2) in dilute AVT(O) solutions, it was found that the corrosion currents for the system of interest are relatively low (see Section 4.1). There are literature data indicating that ENA might be difficult to implement at low corrosion currents, because the magnitudes of the current and the noise are comparable. Taking into account that very dilute electrolyte solutions should be used for the AVT treatment and the corrosion rates expected would be low, a decision was made to first focus the efforts on the DC polarization and EIS methods and to postpone ENA until a later stage of the study.

In a future project, the design of the electrochemical noise (EN) sensor will be based on previous corrosion studies using ENA [16]. The EN sensor assembly in that study included stainless steel wires for both working and counter electrodes. However, the target material used in this project (SA210A1) is not manufactured in the wire form, and the standard sample shape machined from the available tubing is a cylindrical rod (3 mm OD). Taking into account this geometrical limitation, the design of the EN sensor will be modified.

3.5 Steel Specimens

The mild carbon steel SA210A1 is used as a target material in this corrosion study. Samples of the boiler tubes (L=5 ft, OD=1 in., ID=0.6 in.) were obtained from the Boiler Tube Company of America (506 Charlotte Highway, Lyman, SC 29365) along with the chemical specification on the material (Appendix A). Carbon steel rods (L=50 mm, OD=3 mm) were machined out of the tube wall at the Machine Shop of the College of Earth and Mineral Sciences at Penn State University. These rods were carefully polished using sandpaper and extensively cleaned prior to use in the corrosion experiments. The above-mentioned specimens were used as (1) working electrodes in the high temperature working/counter electrode assembly, (2) rotating disk electrode tips in preliminary ambient temperature tests in RDE-2 system, and (3) samples for the mass loss tests.

3.6 Preparation of Solutions

All solutions in these corrosion studies were prepared using ultrapure de-ionized water with resistivity of 18.2 MΩ.cm (Mili-Q water). The solution tank is initially filled and permanently kept under argon atmosphere, and the pH of the working solution is monitored via sampling through a side outlet. A schematic of the used solution supply connected to the high temperature electrochemical cell is shown in Figure 3-8.

A dilute deoxygenated NaCl + NH_4OH aqueous solution (corresponding to AVT(O) chemical treatment: Cl^- 100 ppb, pH 9) was chosen as the first experimental solution and used throughout Task 1 for testing the measurement tools. The solution composition was based on the targeted AVT specifications and was prepared as follows. First, the test tank was filled by ultrapure de-ionized water with resistivity of 18.2 MΩ.cm (Mili-Q water) under the Ar atmosphere to prevent

its contact with air. The 20-liter test tank was calibrated to measure volume with accuracy ± 0.1 l. Then, 5.7 ml of 10^{-2} mol kg^{-1} NaCl and 3.7 ml of 10^{-1} N NH_4OH (Alfa Aesar standardized solution) were injected to the 20 l Mili-Q water using a syringe. The resulting solution (AVTSol-1) contained 100 ppb of Cl^- ($2.85\ 10^{-6}$ mol kg^{-1} NaCl) and had pH = 9. No sulfate was introduced at this time. The prepared solution was bubbled by Ar (PP argon) and kept in the test tank under Ar cap to prevent its contamination by atmospheric gases. The pH was measured by a Cole Palmer high precision glass electrode at room temperature.

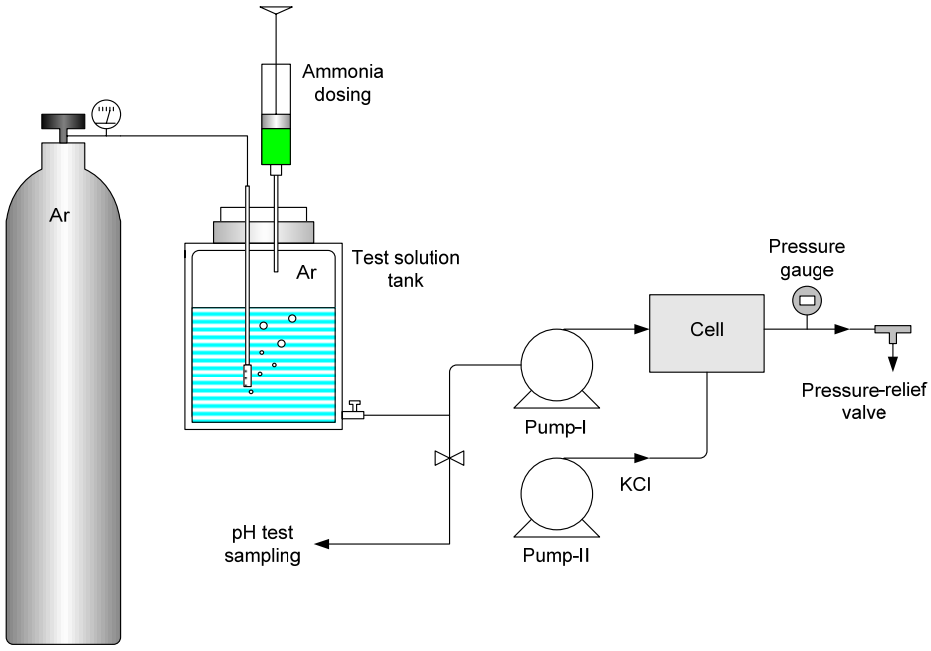

Figure 3-8
Schematic of the Solution Preparation and Supply System

4
RESULTS

4.1 DC Polarization and EIS Measurements

The DC polarization and electrochemical impedance spectroscopy (EIS) are considered the primary methods for the present corrosion study. To verify the workability of the developed tools and to check the appropriateness of the experimental conditions, the measurements were carried out in the following order:

Step 1. The tests were performed using the commercial rotation disk electrode system (RDE-2, BASi) at ambient conditions. In this case, the working electrode is represented by the carbon steel material of interest, and the working solution was an AVT chemistry solution (e.g., AVTSol-1, see Section 3.6). The purpose of these tests was to prove that the electrochemical methods are suitable for the very dilute solutions of interest and the corrosion rates are measurable.

Step 2. The tests were performed using the designed working/counter electrode assembly in a glass flask at ambient conditions. The same working electrode material and working solution are used as in Step 1. The main purpose of these tests was to check the annular duct design (Figure 3-6) and compare the data obtained from different electrode configurations (RDE-2 vs. annular duct). Also the performance of the flow-through reference electrode was checked.

Step 3. The tests were performed using the designed working/counter electrode assembly in the flow-through hydrothermal electrochemical cell at ambient conditions. The main purpose of this step was to check the workability of the electrochemical circuit of the flow-through cell.

Step 4. The tests were performed using the flow-through hydrothermal electrochemical cell at elevated temperatures and pressures, up to 360°C (680°F) and 26 MPa (3770 psi). The purpose of this step was to track any changes in the system operation due to increasing temperature and pressure and finally to collect experimental data for specified regimes at the target parameters.

This stepwise approach allowed possible experimental problems to be quickly identified and make adjustments to the designed tools and technique. Advancement to the next step occured only when the previous step was successfully completed. In the context of this research, Steps 1–3 were considered auxiliary but necessary for obtaining high quality data in Step 4.

Results

For all types of electrochemical tests, the Gamry electrochemical measurements station was used. During Steps 1 and 2, the compatibility of the working range of the Gamry station in DC105 Corrosion Measurement mode with the actual corrosion current magnitudes was confirmed.

Sub-Step 1: DC polarization measurements using RDE-2 system at ambient temperature.

These measurements were performed at ambient temperature for reference. The carbon steel specimen was prepared as follows. First, a small cylindrical rod of carbon steel SA210A1 (L 0.12 in., OD 0.12 in.) was washed and immersed in 0.1 N HCl for half an hour at room temperature. Then the specimen was washed again with distilled water and inserted into the blank RDE tip to be used as a custom working electrode. The surface of the prepared rotating disk electrode was polished by alumina suspension using a standard procedure.

A series of RDE-2 experiments with the SA210A1 carbon steel in AVTSol-1 solution verified the acceptability of the DC polarization and EIS methods for the corrosion studies in very dilute solutions. The Tafel curves obtained have a theoretical shape and are suitable for data fitting and corrosion current calculation. Also the applicability of the two-electrode and three-electrode schemes for the DC polarization measurements was tested. In the two-electrode scheme, the counter and reference electrodes are presented by the same electrode. Some experimental results from Step 1 are presented in Appendix B.

Sub-Step 2: DC polarization measurements using the annular duct working/counter electrode assembly at ambient temperature.

As the next step, the DC polarization measurements were also performed using the flow-through working/counter electrode assembly with annular duct geometry (Figure 3-6). The first measurements were made in a glass flask at the ambient temperature and at different flow rates of AVTSol-1 solution through the system. Two different reference Ag/AgCl electrodes were used for these measurements. The first reference electrode was a commercial standard reference electrode (supplied with the RDE-2 system); the second reference electrode was made in the laboratory and was similar to that to be used in the flow-through setup in the following high temperature studies. The shape of the Tafel curves obtained was well-defined (similar to data in Appendix B) and appropriate for theoretical fitting and determination of targeted corrosion properties. These results confirmed that the newly designed working/counter electrode assembly is suitable for the corrosion current measurements of the SA210A1 carbon steel in very dilute aqueous solutions specified for AVT treatment.

Sub-Step 3: DC polarization and EIS measurements in the flow-through electrochemical cell at ambient temperature.

In this step, the above-described annular duct working/counter electrode assembly and the flow-through Ag/AgCl reference electrode were installed inside the flow-through high temperature electrochemical cell for further testing. Both two-electrode and three-electrode schemes were used in DC polarization measurements. Even though the third (counter) electrode is normally

required to avoid polarization of the reference electrode in current measurements, the two-electrode scheme (with steel working electrode and gold foil counter/reference electrode) used in parallel can also be very useful. In this case, the distance between the electrodes is minimal, which significantly reduces data scattering and improves the accuracy of data treatment. The possibility of using the two-electrode scheme in DC polarization measurements is supported by the fact that in oxygen-deprived solutions (like AVTSol-1), hydrogen is produced at the cathode (Equation 2-9), and at a constant pH the potential of the gold counter electrode remains relatively constant. Such a low polarizable counter electrode can be simultaneously used as a reference electrode in two-electrode DC polarization measurements. The corrosion currents measured with three-electrode and two-electrode methods were found to be in close agreement. However, only the three-electrode scheme is suitable for corrosion potential measurements. The potentiometric measurements performed using the carbon steel working electrode and Ag/AgCl reference electrode yielded stable and reproducible values. The two-electrode scheme was also used for EIS measurements in the flow-through electrochemical cell, because in the case of an AC signal, the polarization of the electrodes is minimal, and the corrosion current can be correctly estimated.

Sub-Step 4: DC polarization and EIS measurements in the flow-through apparatus up to 360°C (680°F).

The corrosion measurements in the temperature range 20–360°C (68–680°F) in the flow-through electrochemical cell were performed using the two-electrode scheme, in which the carbon steel rod was the working electrode, and the gold cylinder played the role of both counter and reference electrode at the same time. It was found that the use of the external Ag/AgCl reference electrode for DC polarization measurements is not quite appropriate in the case of very dilute solutions. The reference NaCl electrolyte flow becomes significantly diluted upon entering the cell and unable to provide an electrolyte bridge with the working electrode. The contact is insufficient, which causes significant data scattering. There are several possible solutions to this problem. The first option is the two-electrode scheme, which is appropriate for oxygen-free solutions and which has been successfully tested for DC polarization and EIS measurements at ambient temperatures (Steps 1–3). The second option is the replacement of the external Ag/AgCl reference electrode with an internal flow-through yttria-stabilized zirconia (YSZ) high temperature reference electrode or an internal flow-through Pt(H_2) reference electrode. Both of the replacement options have their own limitations. The solution pH should be precisely controlled to provide a stable potential, and the second option also implies introduction of hydrogen to the system, which is not desirable in high ORP regimes. The reference electrode replacement will be necessary for future corrosion studies under AVT and OT conditions, and the prospective designs are under development. Nevertheless, application of the external flow-through Ag/AgCl reference electrode to corrosion potential (potentiometric) measurements was successful.

Treatment of the EIS data obtained by the two-electrode method yields two important resistance values: (1) resistance (conductivity) of the electrolyte solution between two electrodes (i.e., between the steel and gold electrodes in the annulus duct), and (2) charge transfer resistance, which (in case of corrosion) should be mainly attributed to the electrochemical process on the steel electrode. From the electrolyte solution conductivity, the electrolyte concentration *in situ*

can be estimated, and this opportunity should be addressed in a separate study. The conductivity measurement was very important for these studies. In this system, in addition to a very dilute AVT solution flowing through the working/counter electrode assembly (Port 1 in Figure 3-2), there was the flow of 0.1 mol kg^{-1} NaCl solution, which occurred in the perpendicular direction through the Ag/AgCl electrode (Port 2 in Figure 3-2). Since the working and reference solutions had a significant composition gradient, some contamination of the working solution due to a thermal convection process or solution pulsation caused by pumping was a potential threat. Therefore, at all experimental temperatures, the working solution quality was controlled with high precision using the EIS technique, which indicated the resistance of the solution in the vicinity of the working electrode. The working solution flow rate (AVTSol-1) through the working electrode was set constant at 1, 5, or 8 $cm^3 min^{-1}$. When the Ag/AgCl reference electrode was used, the flow rate of the NaCl reference solution was kept low enough to avoid contamination of the working solution.

The EIS, DC polarization, and corrosion potential measurements were carried out at several temperatures within the range 20–360°C (68–680°F). A typical cycle of data acquisition at each temperature consisted of the following steps: (1) EIS measurements (two-electrode), (2) corrosion potential measurements (with Au reference electrode), (3) DC polarization measurements (two-electrode), (4) corrosion potential measurements (with Ag/AgCl reference electrode), (5) DC polarization measurements (three-electrode), and (6) EIS measurements (three-electrode). This cycle was repeated until the steady-state values were obtained from the two-electrode EIS tests.

Two representative (steady-state) DC polarization curves obtained at different temperatures are shown in Figure 4-1. The relative position (upward shift) of the high temperature curve indicates an increase of the corrosion current with increasing temperature. A representative Nyquist plot obtained from the EIS measurements at 320°C (608°F) is presented in Figure 4-2. These data were subject to further treatment in the impedance model to retrieve the corrosion current.

4.2 Determination of the Corrosion Current

The DC polarization data collected from different testing steps for the SA210A1 carbon steel material and the AVTSol-1 solution were fitted to the Butler-Volmer type equation (12).

The parameters determined from the experiments using the RDE-2 system (Step 1) and annular duct working/counter electrode assembly at ambient conditions (Step 2) are listed in Table 4-1.

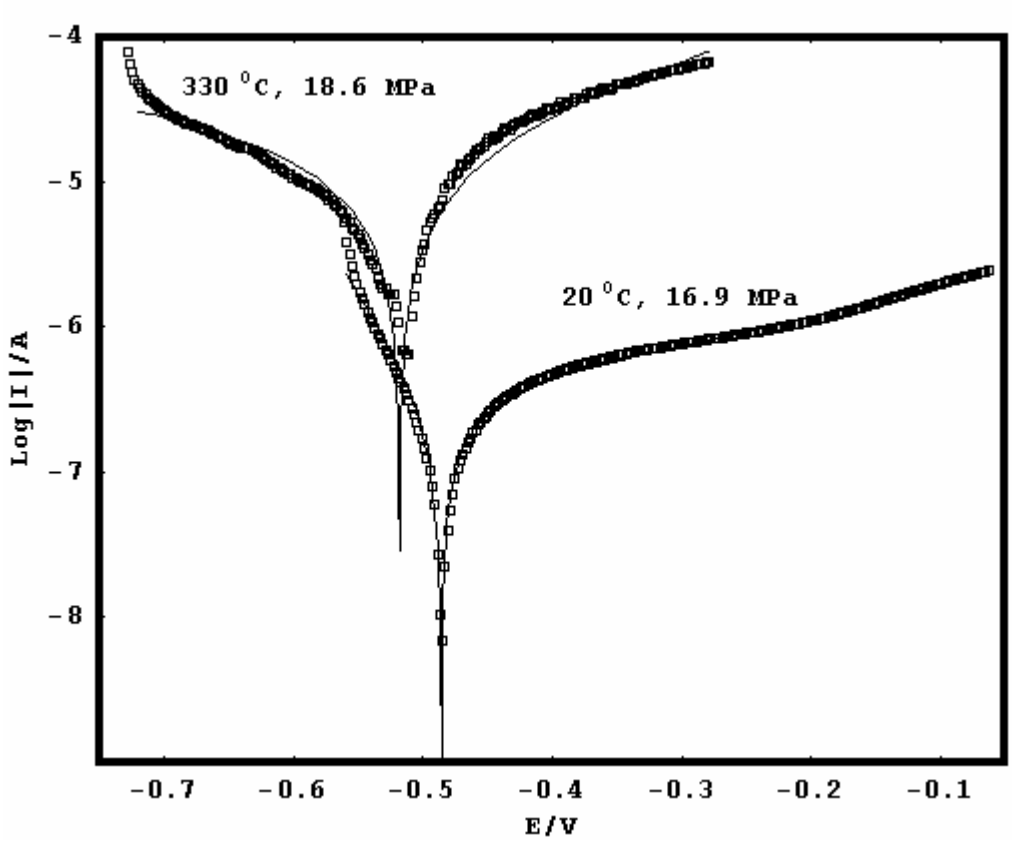

Figure 4-1
DC Polarization Data (Runs *ah61t* and *ah104t*), for SA210A1 Carbon Steel in AVTSol-1 Solution at 20 and 330°C (68 and 626°F)

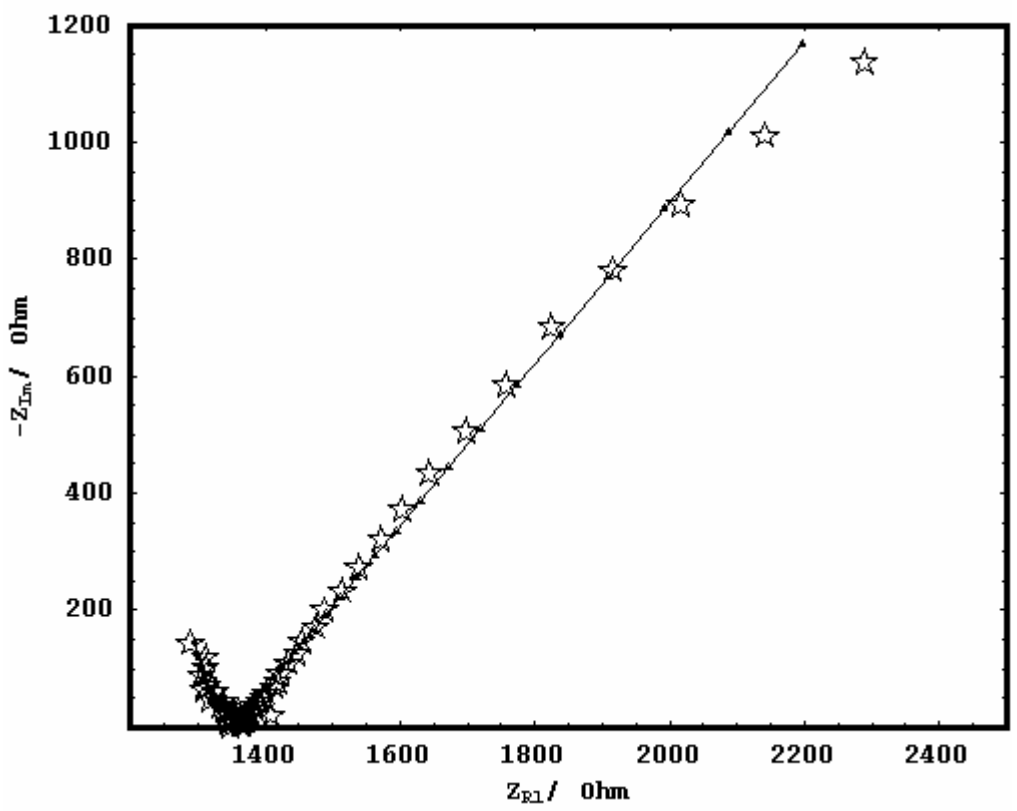

Figure 4-2
EIS Data (Run *ah27i*) for SA210A1 Carbon Steel in the Aqueous Solution AVTSol-1 at 320°C (608°F)

As seen from Table 3-1, the disk rotation provides more intense exposure of the working electrode material to the solution than a channel flow and therefore results in higher corrosion rates at the ambient conditions. The flow rate variation in the flow-through electrode assembly did not cause any systematic changes in corrosion parameters. In the range of relatively slow flow rates, the effect of the flow rate on the corrosion parameters was found to be negligible at 23°C (73°F).

Table 4-1
Corrosion Current, Corrosion Potential, and Charge Transfer Coefficients for SA210A1 Carbon Steel in AVTSol-1 Solution (NaCl + NH_4OH: 100 ppb of Cl^- and pH=9) Determined by DC Polarization Measurements at 23°C (73°F)

Run #	I_{corr} /A	E_{corr} /V	α_1	α_2	Comments
avtrde3	4.57·10-6	-0.59	0.068	0.042	RDE-2, 500 RPM
il7	5.29·10-7	-0.48	0.095	0.144	w/c*, RDE ref. electrode, flow = 5 cm^3 min^{-1}
il9	5.63·10-7	-0.49	0.108	0.178	w/c, RDE ref. electrode, flow = 2.5 cm^3 min^{-1}
il11	7.41·10-7	-0.50	0.096	0.167	w/c, RDE ref. electrode, flow = 0.5 cm^3 min^{-1}
il14	*4.41·10-7*	*-0.55*	*0.168*	*0.283*	w/c, exp. ref. electrode, flow= 1.0 cm^3 min^{-1}

Note: * w/c denotes working/counter electrode assembly with annular duct geometry.

The parameters determined from the experiments in the flow-through electrochemical cell at ambient and elevated temperatures (Steps 3 and 4) are listed in Table 4-2.

Table 4-2
Corrosion Current, Corrosion Potential, and Charge Transfer Coefficients for SA210A1 Carbon Steel in AVTSol-1 Solution (NaCl + NH_4OH: 100 ppb of Cl^- and pH=9) Determined by DC Polarization Measurements at 20–360°C (68–680°F)

Run #	T/°C	T/°F	P/ MPa	I_{corr} /A	E_{corr} /V	α_1	α_2	Flow rate/ cm^3 min^{-1}
ah104t	20	68	16.9	$3.1\cdot10^{-7}$	-0.49	0.06	0.36	5
ah103t	22	72	17.2	$4.0\cdot10^{-7}$	-0.57	0.05	0.34	5
ah87t	200	392	21.6	$1.7\cdot10^{-6}$	-0.36	0.17	0.23	8
ah83t	204	399	21.7	$2.1\cdot10^{-6}$	-0.45	0.16	0.21	8
ah78t	290	554	20.7	$2.1\cdot10^{-6}$	-0.46	0.21	0.32	1
ah80t	297	567	21.7	$2.7\cdot10^{-6}$	-0.52	0.21	0.20	8
ah64t	340	644	18.2	$2.1\cdot10^{-6}$	-0.22	0.20	0.64	1
ah91t	340	644	21.9	$2.4\cdot10^{-6}$	-0.24	0.19	0.37	8
ah94t	360	680	26.1	$2.8\cdot10^{-6}$	-0.23	0.10	0.37	8
ah100t	360	680	25.1	$6.0\cdot10^{-6}$	-0.21	0.13	0.20	8

Results

The EIS data were fitted by the Electrochemical Circuit Cell Model with six parameters: cell capacity, Warburg-Fricke impedance, double electric layer (DEL) capacity (C_{DEL}), solution resistance (R_{SOL}), and charge transfer resistance (R_{CT}). The value of the corrosion current can be estimated from R_{CT} according to the Stern-Geary type equation:

$$I_{CORR}^{CT} \approx \frac{RT}{zFR_{CT}} \quad , \qquad \textbf{Equation 4-1}$$

and the parameters determined from this fitting are presented in Table 4-3.

Table 4-3
Corrosion Charge Transfer Resistance, Double Electric Layer Capacity, and Corrosion Current for SA210A1 Carbon Steel in AVTSol-1 Solution (NaCl + NH_4OH: 100 ppb of Cl^- and pH=9) Determined by EIS Measurements at 20–360°C (68–680°F)

Run #	T/°C	T°F	P / Mpa	R_{SOL} / Ohm	R_{CT} / Ohm	C_{DEL} / F	I_{CORR}^{CT} / A	Flow rate
ah6i	20	68	4.8	15000	2000	$4.6 \cdot 10^{-8}$	$6.2 \cdot 10^{-6}$	5
ah122i	21	70	17.2	11000	2040	$1.0 \cdot 10^{-8}$	$6.2 \cdot 10^{-6}$	5
ah12i	100	212	10.3	3000	840	$1.5 \cdot 10^{-9}$	$1.9 \cdot 10^{-5}$	5
ah112i	204	399	21.6	3700	490	$3.0 \cdot 10^{-8}$	$4.2 \cdot 10^{-5}$	8
ah111i	205	401	21.5	3000	340	$3.0 \cdot 10^{-8}$	$6.0 \cdot 10^{-5}$	5
ah103i	321	610	21.7	2980	200	$2.0 \cdot 10^{-7}$	$1.3 \cdot 10^{-4}$	8
ah115i	330	626	21.9	3790	730	$1.0 \cdot 10^{-8}$	$3.5 \cdot 10^{-5}$	8
ah100i	336	637	21.7	2370	250	$2.0 \cdot 10^{-7}$	$1.1 \cdot 10^{-4}$	5
ah101i	344	651	21.7	3140	210	$6.0 \cdot 10^{-5}$	$1.3 \cdot 10^{-4}$	8
ah102i	356	673	21.7	3300	580	$1.0 \cdot 10^{-8}$	$4.7 \cdot 10^{-5}$	8
ah117i	360	680	26.0	3670	320	$5.0 \cdot 10^{-8}$	$1.1 \cdot 10^{-4}$	8
ah119i	360	680	26.2	4270	270	$1.0 \cdot 10^{-6}$	$1.0 \cdot 10^{-4}$	8

The overall temperature dependence of the corrosion currents obtained by DC polarization and EIS methods is illustrated in Figure 4-3. The DC polarization data points represent the averaged corrosion currents from several measurements run at close temperatures. The general tendency indicates that the rate of corrosion of SA210A1 carbon steel in AVTSol-1 solution should increase by more than an order of magnitude as the temperature increases from 20 to 360°C (68 to 680°F). The difference in the magnitude of the corrosion currents obtained by these two methods is explained by a different character of polarization (see Equations 2-14 to 2-16). As a result, the corrosion currents measured by EIS are higher than those measured by DC polarization. The DC polarization measurements are influenced by the changes in electrode surface areas occupied by anodic and cathodic cells due to the changes of the electric field.

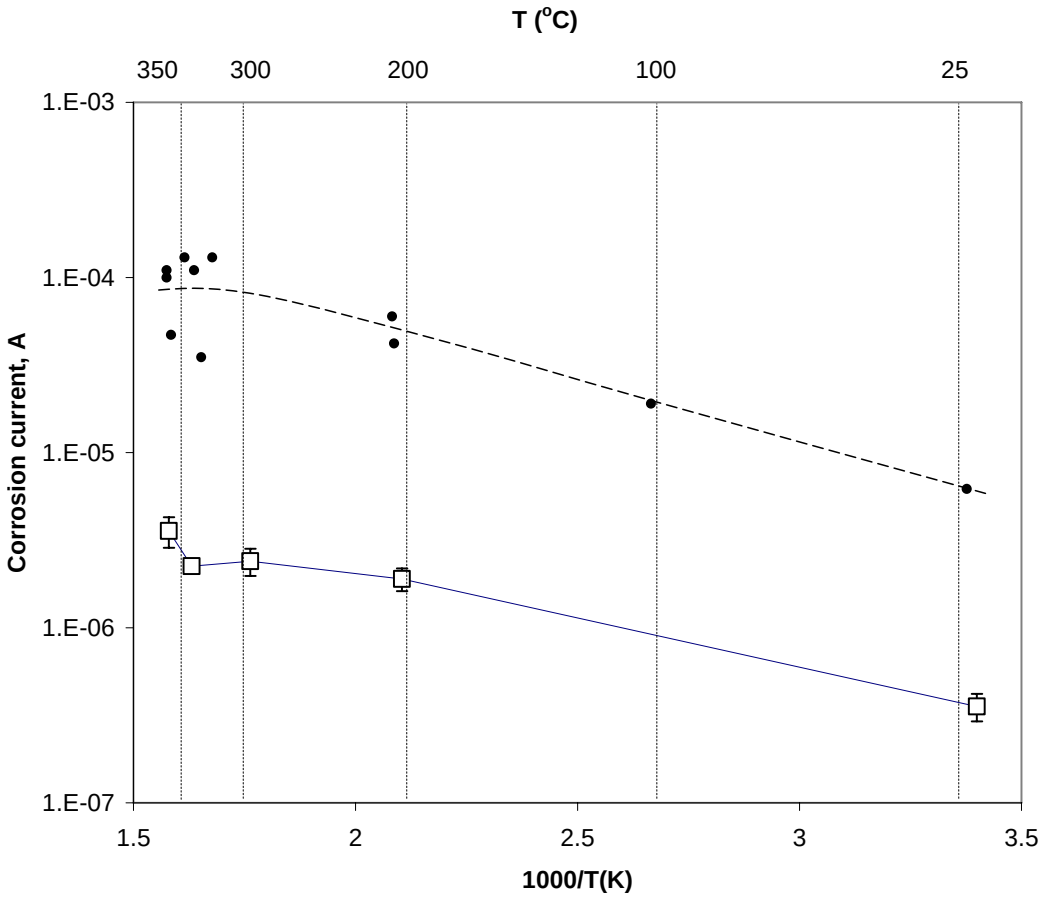

Figure 4-3
Corrosion Current Measured by DC Polarization (Squares) and EIS (Dots) for SA210A1 Carbon Steel in AVTSol-1 Solution as a Function of Temperature

4.3 Corrosion Product Analysis

The mass loss tests are considered a complementary but important part of this corrosion research. Due to the well established approach to calculate the corrosion rate from the mass loss experimental data [43], this method is usually used throughout the study to confirm the *in situ* electrochemical methods and obtain the most complete information on the corrosion kinetics. Since the experimental time for a mass loss test is considerably longer than that required for an electrochemical experiment, the mass loss tests were planned only for the main representative conditions.

The average corrosion rate of a material specimen can be found as follows:

$$\text{Corrosion rate} = \frac{\Delta M}{A \times t \times \rho_S} \qquad \textbf{Equation 4-2}$$

where ΔM is the mass change during mass loss test, A is the initial surface area of the specimen, t is the time of exposure, and ρ_S is the material density. While operating in the same units, the corrosion rate can be alternatively found from an electrochemical experiment as follows:

$$\text{Corrosion rate} = \frac{I_{corr} M_w^{Me}}{AzF\rho_s} \qquad \textbf{Equation 4-3}$$

where I_{corr} is the corrosion current, z is the oxidation number, F is the Faraday constant, and M_w^{Me} is the atomic mass of metal. The corrosion rate measured by an electrochemical method corresponds to the instantaneous condition of the system, while the corrosion rate determined via mass loss test yields the total average rate over the experimental time. To obtain an adequate comparison of the experimental data, the times of the electrochemical and mass loss tests should coincide at some point. Also the mass loss tests should be performed for several representative times, so that the kinetic curve could be extrapolated. Corrosion rates are not necessarily constant with time.

The carbon steel specimen used for the mass loss analysis in this study was identical to the working electrode in the annular duct working/counter electrode assembly. The specimen shape was a cylindrical rod with the dimensions of 3.07 mm OD and 11.51 mm length (dimensions of each specimen were accurately measured prior to the test). The surface area of the specimen was calculated based on cylindrical geometry and was equal to 125.66 mm^2.

The mass loss tests were performed according to the following procedure:

1. The carbon steel specimen was polished with an abrasive paper, rinsed in distilled water, and air dried before the test.
2. The dimensions of the specimen were precisely measured.
3. The specimen was weighed to the fifth significant figure.
4. The specimen was placed inside an alumina ceramic tube, which served as a flow channel for the working solution. The tube was fixed to the high pressure Conax gland via Teflon fittings in the cold zone.
5. The tube with the specimen was installed in the high temperature flow-through cell (the same cell used for electrochemical measurements), and the system was brought to target temperature/pressure conditions.
6. The working solution was continuously pumped through the system at the flow rate similar to that in electrochemical experiments, and the exposure was timed.
7. After the experiment, the specimen was removed from the flow channel and examined.
8. The loose corrosion products were mechanically removed from the specimen surface and kept for analysis.

9. The specimen was subjected to repeated chemical cleaning. Following the ASTM recommendations [43], the cleaning solution contained 500 ml HCl (density 1.19 g cm^{-3}), 3.5 g of crystalline hexamethylene tetramine, and pure water to make 1000 ml. The specimen was rinsed in solution with rigorous stirring for 10 min at room temperature.
10. The specimen was weighed to the fifth significant figure.

In the above procedure, Steps 9 and 10 were repeated several times until the weight of the specimen was constant or the slope of the weight change vs. number of treatments decreased sharply, indicating that no more corrosion products could be removed. The mass loss recorded in Step 10 was used for the corrosion rate calculation.

The mass loss test for the SA210A1 carbon steel in the AVTSol-1 solution was performed according to the procedure outlined above. The experimental parameters were 300°C (662°F) and 20 MPa. After the experiment, the surface of the steel specimen was covered by a black powdery layer (presumably magnetite), most of which could be easily wiped off. After removal of the loose corrosion product, the specimen still had a black tint due to the dense coating layer on its surface. This dense corrosion layer dissolved after several washings in the above-described cleaning reagent.

The specimen properties used in the mass loss experiment are listed in Table 4-4.

Table 4-4
Parameters of the Mass Loss Experiments for SA210A1 Carbon Steel in AVTSol Solution and Calculated (Equation 4-2) Corrosion Rates

Specimen	SA210A1
Pre-oxidation	No
Mass (g) before experiment	0.61656
Surface area (mm^2)	125.66
Mass (g) after experiment	0.61318
Mass loss (g)	0.00338
Exp. time	120 hours
T(average),°C (°F)	300 (572)
P, MPa	20
Corrosion rate (mm $year^{-1}$)	0.25

The total mass change of the specimen after the removal of corrosion products (0.00338 g) corresponded to a corrosion rate of 0.25 mm/year. The comparison of the corrosion rates obtained by different methods for the AVT(O) treatment is given in Section 4.4.

In the future studies, it is planned to study the morphology and composition of the corrosion products on the surface of the carbon steel specimens using SEM-EDS analysis. Fresh (uncorroded) specimens will be analyzed in parallel for comparison.

4.4 Determination of Optimum Chemistry and Bounding Limits for AVT

4.4.1 Background

Feedwater chemistry is a primary factor affecting boiler reliability. AVT is one of the treatment regimes used to protect the boiler materials and to reduce the corrosion levels in fossil plants. The main feature of the AVT treatment is an elevated pH, which is achieved by adding ammonia to the system. Two different types of AVT treatment are used in practice, depending on plant specifics: (1) reducing all-volatile treatment AVT(R) and (2) oxidizing all-volatile treatment AVT(O). Oxygenated treatment (OT) can also be used for all-ferrous feedwater systems.

The AVT(R) regime implies the use of a reducing agent, such as hydrazine, and is considered the only suitable treatment for mixed-metallurgy feedwater (e.g., iron/copper). In all-ferrous systems, AVT(R) is very efficient in removal of corrosion products, such as iron oxides (magnetite, hematite) via reduction. Addition of the reducing agent is combined with the minimization of the air in-leakage to keep the oxygen levels in the system below 10 ppb. In this case, the oxidation-reduction potential (ORP) is significantly less than 0 mV.

The AVT(O) regime does not contain any reducing agent, but the oxygen levels are still kept low (<10 ppb). It was found that, in some cases, eliminating the reducing agent reduces the corrosion product generation. In this treatment, the ORP is not strictly controlled and expected to be around 0 mV.

The OT regime implies the use of high purity oxygenated water. The success of this treatment in ferrous systems is due to the passivation of the metal surface with a ferric oxide hydrate (FeOOH) film. FeOOH has much lower solubility than Fe_3O_4. The ORP is not strictly controlled but is expected to be around +100–150 mV.

The AVT(O) and OT regimes are applicable only in all-ferrous systems. Based on the main requirements for the above-described feedwater treatments, the experimental parameters were determined for Task 2 (Table 4-5). The matrix of targeted chloride/sulfate concentrations for the experimental solution is given in Table 4-6.

Table 4-5
Parameters Ranges Chosen for the Electrochemical Corrosion Measurements under AVT Regime

Parameter	AVT(O)	AVT(R)	OT
pH at 25°C (77°F)	9.2–9.6	9.2–9.6	9.2–9.6
NH_4OH	Yes	Yes	Yes
Reducing agent	No	Hydrazine	No
ORP	~0 mV	-350 mV	~+100-150 mV
Cl^-	0–200 ppb	0–200 ppb	0–200 ppb
SO_4^{-2}	0–400 ppb	0–400 ppb	0–400 ppb
Cl^-/SO_4^{-2}	0.1–10 (mole ratio)	0.1–10 (mole ratio)	0.1–10 (mole ratio)
T	350°C (662°F)	350°C (662°F)	350°C (662°F)
P	18 MPa	18 MPa	18 MPa
Pre-oxidation at lower T	Yes/No	Yes/No	Yes/No

The solution preparation approach and experimental tools, including protection from the influence of atmospheric CO_2 and oxygen, was described in Section 3.6. Preparation and dosing of the NaCl and Na_2SO_4 solutions for chloride and sulfate control followed the standard analytical methods. The pressure/temperature parameters of the AVT treatment specified in Table 4-5 are chosen close to the liquid-vapor equilibrium line for water, and applied pressure ensures the liquid phase for electrochemical studies.

Table 4-6
Matrix of the Cl^-/SO_4^{-2} Mole Ratios of Interest in the AVT Corrosion Study

$mol.kg^{-1}$	Cl^-	0.0E+00	4.2E-07	2.8E-06	5.6E-06
SO_4^{-2}	ppb	0	15	100	200
0.0E+00	0		∞	∞	∞
5.6E-07	54	0	0.75	5.02	10.04
1.0E-06	100	0	0.41	2.71	5.42
2.1E-06	200	0	0.20	1.36	2.71
4.2E-06	400	0	0.10	0.68	1.36

Results

4.4.2 Corrosion Rates for SA210A1 Carbon Steel under AVT(O) Treatment

The work on this task has been started. The first experimental results obtained at temperatures up to 360°C (680°F) served both Task 1 and Task 2 of this project. The solution composition representative of the AVT(O) treatment was chosen for verification of the experimental techniques and testing the designed measurement tools. The quality of these results was taken as a criterion for accomplishment of Task 1.

The first regime tested was AVT(O). The method of solution preparation is described in Section 3.6, and the experimental parameters used are listed in Table 4-7.

The electrochemical data of DC polarization and EIS obtained for the AVT(O) regime are presented in Sections 4.1 and 4.2. The experimentally determined corrosion currents (Tables 4-1 to 4-3) can be re-calculated to corrosion rates (in mm year^{-1}) as follows:

$$R_{CORR} = 10NSY\frac{I_{CORR}M_w^{Fe}}{A_w zF\rho_S}, \qquad \textbf{Equation 4-4}$$

where A_w is the surface area of the working electrode (cm^2), ρ_S is the density of steel material (g cm^{-3}), M_w^{Fe} is the atomic mass of Fe (55.85 g mol^{-1}), and NSY is the number of seconds per year (s year^{-1}). In this study, A_w =1.2 cm^2, ρ_S = 7.84 g cm^{-3}, and thus the experimental corrosion currents can be converted into corrosion rate as $R_{CORR} = 9726.3\,I_{CORR}$. Also the corrosion standard rate can be found from the corrosion current density (A cm^{-2}) as $R_{CORR} = 11641.9\ (I_{CORR} / A_w)$.

Table 4-7
Experimental Parameters and Solution Specification for the First Corrosion Test on SA210A1 Carbon Steel under AVT(O) Conditions

Solution ID: AVTSol-1	
pH at 25°C (77°F)	9.0
NH_4OH	Yes
Reducing agent	No
ORP	Unspecified (~0 mV)
Cl^-	100 ppb
SO_4^{-2}	0 ppb
Cl^-/SO_4^{-2} (mole)	∞
T	20–360°C (68–680°F)
P	18 MPa
Pre-oxidation at lower T	No

The corrosion rates obtained by DC polarization and EIS methods for the SA210A1 carbon steel in the AVTSol-1 solution are given in Tables 4-8 and 4-9, respectively. As was discussed previously, the difference in the corrosion rates indicated by these two methods is attributed to the different character of electrode polarization during the measurements. The corrosion rate measured by mass loss analysis at 300°C (572°F), 0.25 mm year^{-1}, falls in between the values yielded by DC polarization and EIS. Close coincidence of these rates was not expected and would not be correct, because the mass loss test indicates an integral (cumulative) corrosion for the time of specimen exposure. At the same time, the corrosion rates determined from experimentally measured corrosion currents are instantaneous and may be time dependent. Correlation of the corrosion rates produced by different methods is an important task, which will be pursued in 2006 via collection and analysis of additional experimental data.

Table 4-8
Corrosion Rates for the SA210A1 Carbon Steel in the AVTSol-1 Solution Obtained by DC Polarization

Run #	T/°C	T/°F	P/ MPa	I_{corr} /A	Corrosion Rate/mm year^{-1}
ah103t	22	72	17.2	$4.0 \cdot 10^{-7}$	0.004
ah104t	20	68	16.9	$3.1 \cdot 10^{-7}$	0.003
ah87t	200	392	21.6	$1.7 \cdot 10^{-6}$	0.017
ah83t	204	399	21.7	$2.1 \cdot 10^{-6}$	0.020
ah78t	290	554	20.7	$2.1 \cdot 10^{-6}$	0.020
ah80t	297	567	21.7	$2.7 \cdot 10^{-6}$	0.026
ah64t	340	644	18.2	$2.1 \cdot 10^{-6}$	0.020
ah91t	340	644	21.9	$2.4 \cdot 10^{-6}$	0.023
ah94t	360	680	26.1	$2.8 \cdot 10^{-6}$	0.027
ah100t	360	680	25.1	$6.0 \cdot 10^{-6}$	0.058

Table 4-9
Corrosion Rates for the SA210A1 Carbon Steel in the AVTSol-1 Solution Obtained by EIS Measurements

Run #	T/°C	T°F	P / MPa	I_{CORR}^{CT} / A	Corrosion Rate/mm year^{-1}
ah6i	20	68	4.8	$6.2 \cdot 10^{-6}$	0.06
ah122i	21	70	17.2	$6.2 \cdot 10^{-6}$	0.06
ah12i	100	212	10.3	$1.9 \cdot 10^{-5}$	0.37
ah112i	204	399	21.6	$4.2 \cdot 10^{-5}$	0.41
ah111i	205	401	21.5	$6.0 \cdot 10^{-5}$	0.58
ah103i	321	610	21.7	$1.3 \cdot 10^{-4}$	1.26
ah115i	330	626	21.9	$3.5 \cdot 10^{-5}$	0.34
ah100i	336	637	21.7	$1.1 \cdot 10^{-4}$	1.07
ah101i	344	651	21.7	$1.3 \cdot 10^{-4}$	1.26
ah102i	356	673	21.7	$4.7 \cdot 10^{-5}$	0.46
ah117i	360	680	26.0	$1.1 \cdot 10^{-4}$	1.07
ah119i	360	680	26.2	$1.0 \cdot 10^{-4}$	0.97

Table 4-10 provides a general comparison of the corrosion rates determined in this study with some literature data. The published papers cited in this table deal with various materials (steels and alloys) and various electrolyte solutions, most of which are much more concentrated than the solutions used in this study. Nevertheless, such comparison helps to evaluate the overall corrosion situation in the system under study and to illustrate the general tendency of the corrosion rate drift with temperature.

Table 4-10
Comparison of Corrosion Rates (mm year^{-1}) of Different Steels in Different Aqueous Solutions at Some Representative Temperatures

T,°C (°F)	SA210A1 (1)	SA210A1 (2)	SS 304 (3)	Alloy 625 (4)	Mild Steel (5)	CS 1018 (6)	Industrial CS (7)
23 (73)	0.004	0.06			0.05/0.017	0.0076	0.038/0.014
100 (212)		0.37					
150 (302)			0.12				
200 (392)	0.017	0.40	3.5				
300 (572)	0.026		35	44			
360 (680)	0.034	1.02					

(1) – Data of this report: AVTSol-1 solution (Table 4-7), DC polarization method; the values are interpolated for the tabulated temperatures.

(2) – Data of this report: AVTSol-1 solution (Table 4-7), EIS method; the values are interpolated for the tabulated temperatures.

(3) – 0.01 mol kg^{-1} HCl + 0.1 mol kg^{-1} NaCl(aq) solution saturated with H_2 at 25°C (77°F) [16];

(4) – 0.05 – 0.2 mol kg^{-1} HCl(aq) or H_2SO_4(aq) solutions [3];

(5) – 3.5% NaCl(aq) solution; mass loss (upper) / corrosion current (lower) measurements [40];

(6) – Oxygenated or nitrogenated pond water solutions [41];

(7) – 10^{-3} mol kg^{-1} NH_4OH(aq) solution; mass loss (upper) / electrochemical (lower) measurements [42].

5
CONCLUSIONS

1. The experimental tools for electrochemical corrosion measurements up to 360°C (680°F), including a hydrothermal cell, an annular duct flow-through working/counter electrode assembly, and flow-through external Ag/AgCl reference electrode were designed and tested.

2. The DC polarization two-electrode and three-electrode techniques showed the highest promise for the corrosion rate measurements in the dilute electrolyte solutions of interest.

3. The electrochemical impedance spectroscopy (EIS) method provided the upper limit values for the instantaneous corrosion currents and can also be used as an efficient tool to control the juvenility of the working solution in the flow-through cell using high temperature conductivity measurement.

4. The applicability of the external flow-through Ag/AgCl reference electrode to the DC polarization measurements in very dilute aqueous solutions was considered questionable because of high data scattering. While this electrode proved to be good for corrosion potential measurements, other types of reference electrodes, such as internal flow-through YSZ or Pt(H_2), are being contemplated as alternative options.

5. The corrosion rates of the SA210A1 carbon steel were determined for the case of chloride dominated AVT(O) solution (Cl^- 100 ppb, SO_4^{-2} 0 ppb) in the temperature range from 20°C (68°F) to 360°C (680°F). The first DC polarization and EIS tests showed that the electrochemical corrosion rate increased by more than one order of magnitude with temperature increasing from 20°C (68°F) to 360°C (680°F). These data cover only one composition of the AVT(O) chemical regime (Task 2) and will be further extended to all compositional matrices.

6. The corrosion rate determined from the mass loss test was found to fall in between the corrosion rate values obtained from the DC polarization and EIS methods.

6
FUTURE RESEARCH

Task 1 of this project, involving the development of the methodology and experimental tools, is close to completion. The corrosion measurements of the SA210A1 carbon steel will be continued using the developed methodology under chemical treatments of interest. The two-electrode and three-electrode DC polarization measurements will be considered the main electrochemical technique for determination of the corrosion rate of the steel specimens. The EIS method will be used in parallel to find the maximum corrosion rate (as was described in Section 4.2). The EIS will be routinely used to measure the ionic conductivity of the working solution during the experiment and, thus, to control the juvenility of the solution flow. The mass loss experiments will be performed in a separate experimental system concurrently with the electrochemical measurements. This method will be regarded as auxiliary and will be used to measure the cumulative corrosion over a certain period of time and to provide a reference for the electrochemically measured corrosion parameters. For each chemical treatment regime (AVT, OT, PC, or CT), the mass loss test will be performed only for the solution composition causing the highest corrosion rates.

The electrochemical experiments will be performed in the temperature range 25 to 350°C (77 to 662°F). The experimental runs will be scheduled according to the task matrices given in Tables 6-1 (AVT and OT), 6-2 (PC), and 6-3 (CT). In each run (for each solution composition), the temperature will be changed stepwise, and the measurements at each temperature point will continue for at least 4 days or until the measured corrosion current reaches a plateau. In the regular experiments, the measurements will be started from the highest temperatures, and in pre-oxidation experiments, the measurements will be started from the lower temperatures. The pre-oxidation check in each of these regimes implies that the specimen (carbon steel) will be initially heated in the system to a temperature that is significantly lower than the highest target temperature, presumably 200°C (392°F) and pre-conditioned (pre-oxidized). After the pre-oxidation period, the system will be brought to the temperature of 350°C (662°F), and the electrochemical measurements will be carried out as usual. To ensure a good sensitivity of these checks, the experiments with pre-oxidized specimens will be primarily performed for the solution compositions causing the highest corrosion rates. Analogous pre-oxidation treatments will be carried out in mass loss tests as well.

Table 6-1
Experimental Runs (Numbers) Scheduled for Electrochemical Corrosion Studies for AVT and OT Regimes

T = 25-350°C (77-662°F) P = 18 MPa (2610 psi)	AVT(O) (ORP~0 mV)	AVT(R) (ORP~-300 mV)	OT** (ORP~+150 mV)
Cl^- only (200 ppb)	1	7	-
Cl^- rich (Cl^-/SO_4^{-2} ~10)*	2	8	-
Balanced (Cl^-/SO_4^{-2} ~1)	3	9	13
SO_4^{-2} rich (Cl^-/SO_4^{-2} ~0.1)	4	10	-
SO_4^{-2} only (400 ppb)	5	11	-
Pre-oxidation check	6	12	14

*Given chloride-sulfate molar ratios are approximate and will be calculated for particular runs based on actual reagent doses (in ppb).

**OT regime runs are scheduled together with the AVT regime runs for convenience due to the similar solution chemistry used in both of these treatments.

Table 6-2
Experimental Runs (Numbers) Scheduled for Electrochemical Corrosion Studies for PC Regime

T = 25-350°C (77-662°F) P = 18 MPa (2610 psi)	PC(L) ($[PO_4^{3-}]_{tot}$<3 ppm)	PC(H) ($[PO_4^{3-}]_{tot}$>3 ppm)
Cl^- 150 ppb; SO_4^{-2} 600 ppb	15	-
Cl^- 300 ppb; SO_4^{-2} 1200 ppb	-	17
Pre-oxidation check	16	18

Table 6-3
Experimental Runs (Numbers) Scheduled for Electrochemical Corrosion Studies for CT Regime

T = 25-350°C (77-662°F) P = 18 MPa (2610 psi) Cl^- 300 ppb; SO_4^{-2} 600 ppb	CT
NaOH 0.5 ppm	19
NaOH 1 ppm	20
NaOH 2 ppm	21
Pre-oxidation check	22

According to the specified physicochemical conditions that need to be covered by these studies, at least 22 experiments will be conducted (excluding repeated runs). The proposed time table for the future studies is shown in Table 6-4. The appropriate time necessary for completion of each of the Tasks 2–4 was estimated, taking into account the actual experimental time for each electrochemical and mass loss measurement (at least 4 days) multiplied by the number of temperature points, experiment preparation, maintenance of the experimental systems, processing of results and methodical adjustments, and preparation of reports. This time table does not include repeated experiments for the same conditions and does not consider any unforeseen breakdowns in system operation.

Further development of methodology for high temperature corrosion studies will be continued alongside with the measurements at least for the first quarter of 2006. In particular, a new design of a high temperature electrochemical noise sensor will be developed, and the possibility of using ENA in the very dilute electrolyte solutions will be tested experimentally. Alternative high temperature reference electrodes will be tested for the DC polarization measurements in very dilute solutions. The prospective options are internal flow-through YSZ or/and Pt(H_2) reference electrodes. Ways will be explored to most efficiently correlate electrochemical data with *ex situ* methods (such as mass loss analysis and SEM) and will assess the kinetic aspects of both types of experiments under the conditions of interest.

Table 6-4
Suggested Time Table for the Future Electrochemical Corrosion Studies

Tasks	2006	2007
Methodology development		
AVT		
PC		
CT		
OT		
Data treatment		
Monthly, Annual, and Final Reports		

7
REFERENCES

1. S.N. Lvov, in *Encyclopaedia of Electrochemistry V. 6* (M. Stratmann and A. Bard, Eds.), Wiley-VCH (2005, in press).

2. S.N. Lvov and D.A. Palmer, in *The Physical and Chemical Properties of Aqueous Systems at Elevated Temperatures and Pressures: Water, Steam and Hydrothermal Solutions* (Eds.: D.A. Palmer, R. Fernández-Prini, and A.H. Harvey), Elsevier, Amsterdam, 377-408 (2004).

3. P. Kritzer, *J. Supercrit. Fluids* 29 1-29 (2004).

4. G.G. Wildgoose, D. Giovanelli, N.S. Lawrence, and R.G. Compton, *Electroanalysis* 16 421-433 (2004).

5. D. Giovanelli, N.S. Lawrence, and R.G. Compton, *Electroanalysis* 16: 789-810 (2004).

6. S. D. Cramer and B.S. Covino, (Eds.) *ASM Handbook, Volume 13A, Corrosion: Fundamentals, Testing, and Protection*, ASM International, Materials Park, OH (2003).

7. W. Schmickler, *Interfacial Electrochemistry*, Oxford University Press (1996).

8. S.N. Lvov, H. Gao, D. Kouznetsov, I. Balachov, and D.D. Macdonald, *Fluid Phase Equilibria*, 150-151, p. 515 (1998).

9. S.N. Lvov, X.Y. Zhou, and D.D. Macdonald, *J. Electroanal. Chem.*, 463, p. 146 (1999).

10. L.N. Trevani, E. Calvo, and H.R. Corti, *J. Chem. Soc.*, Faraday Trans, 93 4319-4326 (1997).

11. D.D. Macdonald, J. Mankowski, M. Karaminezhaad-Ranjbar, and Y.-H. Hu, *Corrosion* 44 186-192 (1988).

12. Z. Nagy, L.A. Curtiss, J.W. Halley, J. Hautmann, N.C. Hung, Y.J. Rhee, and R.M. Yonco, *J. Electrochem. Soc.* 138 2032-2041 (1991).

13. C.-Y. Liu, R. Shelly, and A.J. Bard, *J. Phys. Chem.* B 101 1180-1185 (1997).

14. A.C. McDonald, F.-R.F. Fan, and A.J. Bard, *J. Phys. Chem.* 90 196-202 (1997).

15. W.-K. Lai and Z. Szklarska-Smialowska, *Corrosion* 47 40-47 (1991).

16. X.Y. Zhou, S.N. Lvov, X.J, Wei, L.G. Benning, and D.D. Macdonald, *Corrosion Sci.* 44 841 (2002).

17. Electrochemical Measurement System and Software Installation Manuals, Gamry Instruments Inc. (1999).

18. G. Prentice, *Electrochemical Engineering Principles*. New Jersey, Prentice Hall (1991).

19. F. Scholz, *Electroanalytical Methods, Guide to Experiment and Applications*. Berlin, New York, Springer (2002).

20. D.A. Eden, M. Hoffman, and B.S. Skerry, Polymeric Materials for Corrosion Control, ACS Symposium Series 322 36 (1986).

21. C.-T.Chen, and B.S. Skerry, *Corrosion* 47 598 (1991).

22. F. Mansfeld, and H. Xiao, *J. Electrochem. Soc.* 140 2205 (1993).

23. F. Mansfeld, and C.C. Lee, *J. Electrochem. Soc.* 144, 2068 (1997).

24. H Xiao, and F. Mansfeld, *J. Electrochem. Soc.* 141, 2332 (1994).

25. H. Xiao, L.T. Han, C.C. Lee, and F. Mansfeld, *Corrosion* 53, 412 (1997).

26. U. Bertocci, C. Gabrielli, F. Huet, M. Keddam, and P. Pousseau, *J. Electrochem. Soc.* 144, 37 (1997).

27. G. Gusmano, G. Montesperelli, S. Pacetti, and A. D'Amico, *Corrosion* 53 860 (1997).

28. Y.J. Tan, S. Bailey, B. Kinsella, and A. Lowe, *J. Electrochem. Soc.* 147 530 (2000).

29. R.J.K. Wood, J.A. Wharton, A.J. Speyer, and K.S. Tan, *Tribology Intl.* 335 631 (2002).

30. J.G. Yu, and J.L. Luo, *Langmuir* 18 6637 (2002).

31. A.M. Lowe, H. Eren, and S.I. Bailey, *Corrosion Sci.* 45 941 (2003).

32. C. Liu, D.D. Macdonald, E. Medina, J.J. Villa, and J.M. Bueno, *Corrosion* 50 687 (1994).

33. D.D. Macdonald, C. Liu, and M.P. Michael, *ASTM STP* **1277** 247 (1996).

34. M.P. Manahan, Sr., D.D. Macdonald, and A. Peterson, *Corros. Sci*. **37** 189 (1995).

35. Lvov, S.N. and Zhou, X.Y., *Mineral Mag*., v. 62A, p. 929 (1998).

36. S.N. Lvov, X.Y. Zhou, G.C. Ulmer, H.L. Barnes, D.D. Macdonald, S.M. Ulyanov, L.G. Benning, D.E. Grandstaff, M. Manna, and E. Vicenzi, *Chem. Geol*., v. 198, p. 141 (2003).

37. T.K. Ross and A.A. Wragg, *Electrochim. Acta*, **10**, 1093 (1965).

38. V.N. Balashov, Diffusion of Electrolytes in Hydrothermal Systems: Free Solution and Porous Media, in *Fluids in Crust: Equilibrium and Transport Properties*, K.I. Shmulovich, B.W.D. Yardley, and G.A. Gonchar, Eds., New York: Chapman & Hall, p. 215-251 (1995).

39. S.N. Lvov, H. Gao, and D.D. Macdonald, *J. Electroanal. Chem*., 443, 186-194 (1998).

40. C. Bertolotto and A.M. Beccaria, *Corrosion Prevention & Control*, February, p. 7 (1996).

41. D. Tao, G.L. Chen, and B.K. Parekh, *Minerals Engineering*, 18, p. 481 (2005).

42. Samide, I. Bibicu, M.S. Rogalski, and M. Preda, *Corrosion Science*, 47, p. 1119 (2005).

43. Standard practice for preparing, cleaning, and evaluating corrosion test specimens, G1-90, *Annual Book of ASTM Standards*, Section 3, v. 02.02 (2003).

A

VENDOR'S SPECIFICATIONS OF THE CARBON STEEL SA210A1 MATERIAL PROVIDED FOR ELECTROCHEMICAL CORROSION STUDIES

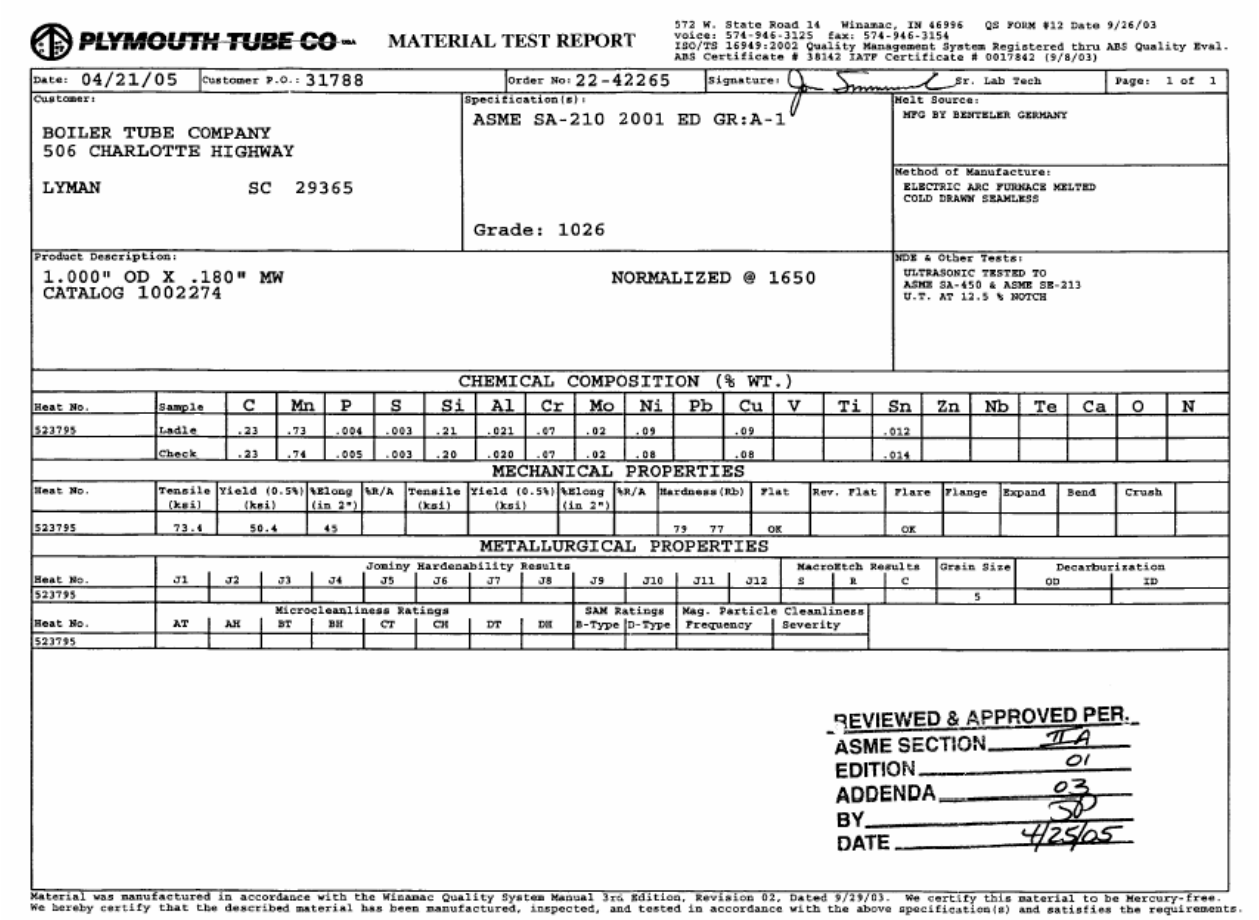

PLYMOUTH TUBE CO. — MATERIAL TEST REPORT

572 W. State Road 14 Winamac, IN 46996 QS FORM #12 Date 9/26/03
voice: 574-946-3125 fax: 574-946-3154
ISO/TS 16949:2002 Quality Management System Registered thru ABS Quality Eval.
ABS Certificate # 38142 IATF Certificate # 0017842 (9/8/03)

Date: 04/21/05 | Customer P.O.: 31788 | Order No: 22-42265 | Signature: Sr. Lab Tech | Page: 1 of 1

Customer:
BOILER TUBE COMPANY
506 CHARLOTTE HIGHWAY
LYMAN SC 29365

Specification(s):
ASME SA-210 2001 ED GR:A-1
Grade: 1026

Melt Source:
MFG BY BENTELER GERMANY

Method of Manufacture:
ELECTRIC ARC FURNACE MELTED
COLD DRAWN SEAMLESS

Product Description:
1.000" OD X .180" MW
CATALOG 1002274
NORMALIZED @ 1650

NDE & Other Tests:
ULTRASONIC TESTED TO
ASME SA-450 & ASME SE-213
U.T. AT 12.5 % NOTCH

CHEMICAL COMPOSITION (% WT.)

Heat No.	Sample	C	Mn	P	S	Si	Al	Cr	Mo	Ni	Pb	Cu	V	Ti	Sn	Zn	Nb	Te	Ca	O	N
523795	Ladle	.23	.73	.004	.003	.21	.021	.07	.02	.09		.09			.012						
	Check	.23	.74	.005	.003	.20	.020	.07	.02	.08		.08			.014						

MECHANICAL PROPERTIES

Heat No.	Tensile (ksi)	Yield (0.5%) (ksi)	%Elong (in 2")	%R/A	Tensile (ksi)	Yield (0.5%) (ksi)	%Elong (in 2")	%R/A	Hardness(Rb)	Flat	Rev. Flat	Flare	Flange	Expand	Bend	Crush	
523795	73.4	50.4	45						79 77	OK		OK					

METALLURGICAL PROPERTIES

Heat No.	Jominy Hardenability Results J1	J2	J3	J4	J5	J6	J7	J8	J9	J10	J11	J12	MacroEtch Results S	R	C	Grain Size	Decarburization OD	ID
523795																5		

Heat No.	Microcleanliness Ratings AT	AH	BT	BH	CT	CH	DT	DH	SAM Ratings B-Type	D-Type	Mag. Particle Cleanliness Frequency	Severity
523795												

REVIEWED & APPROVED PER:
ASME SECTION IIA
EDITION 01
ADDENDA 03
BY
DATE 4/25/05

Material was manufactured in accordance with the Winamac Quality System Manual 3rd Edition, Revision 02, Dated 9/29/03. We certify this material to be Mercury-free.
We hereby certify that the described material has been manufactured, inspected, and tested in accordance with the above specification(s) and satisfies the requirements.

B
COMPARISON OF THE THREE-ELECTRODE AND TWO-ELECTRODE SCHEMES OF EIS AND DC POLARIZATION MEASUREMENTS USING THE RDE-2 SYSTEM

The Tafel curves for two-electrode and three-electrode schemes are shown in Figure B-1 and Nyquist plots for both cases in Figure B-2. The three-electrode Tafel curve and EIS data were taken first. The two-electrode DC polarization curve and EIS were taken after 1.5 hours in the same solution AVTSol-1. In both cases, the RPM was equal to 260. The results of the data treatment are presented in Tables B-1 and B-2.

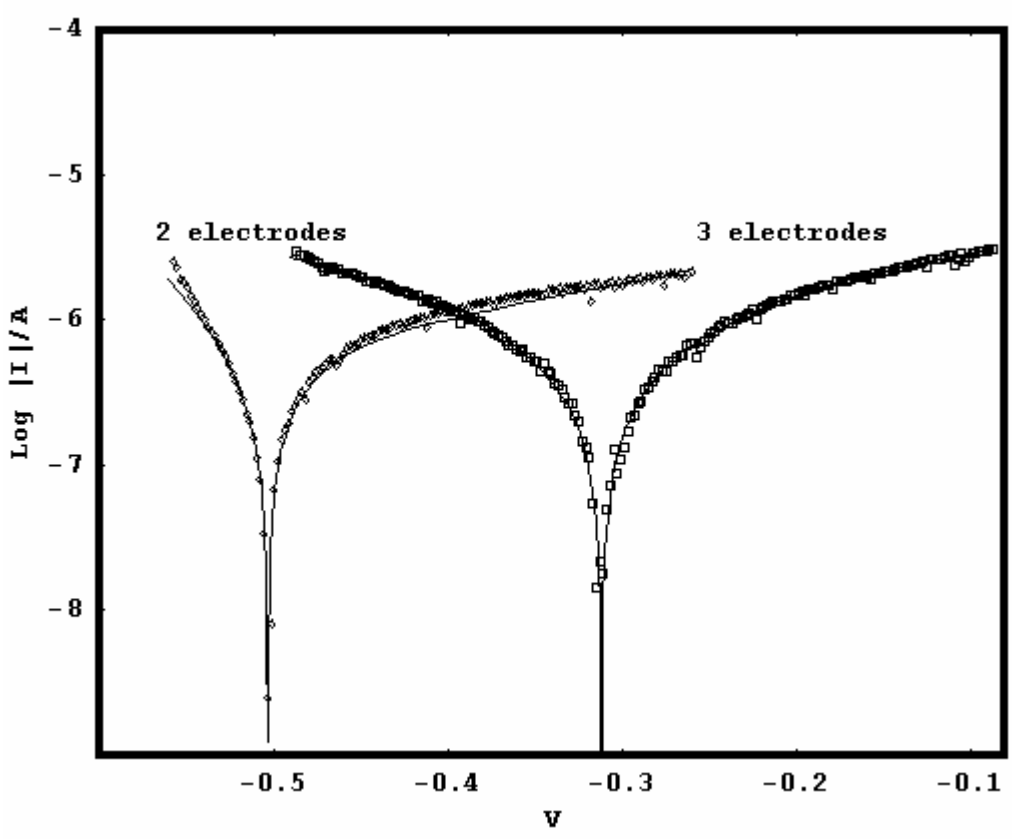

Figure B-1
Comparison of DC Polarization for the Different Electrodes Schemes: AVTSol-1, RDE-2 at 23°C (73°F) (Runs *ard11t* and *ard12t)*. The Solid Lines Correspond to the Data Fitting by Equation 2-12.

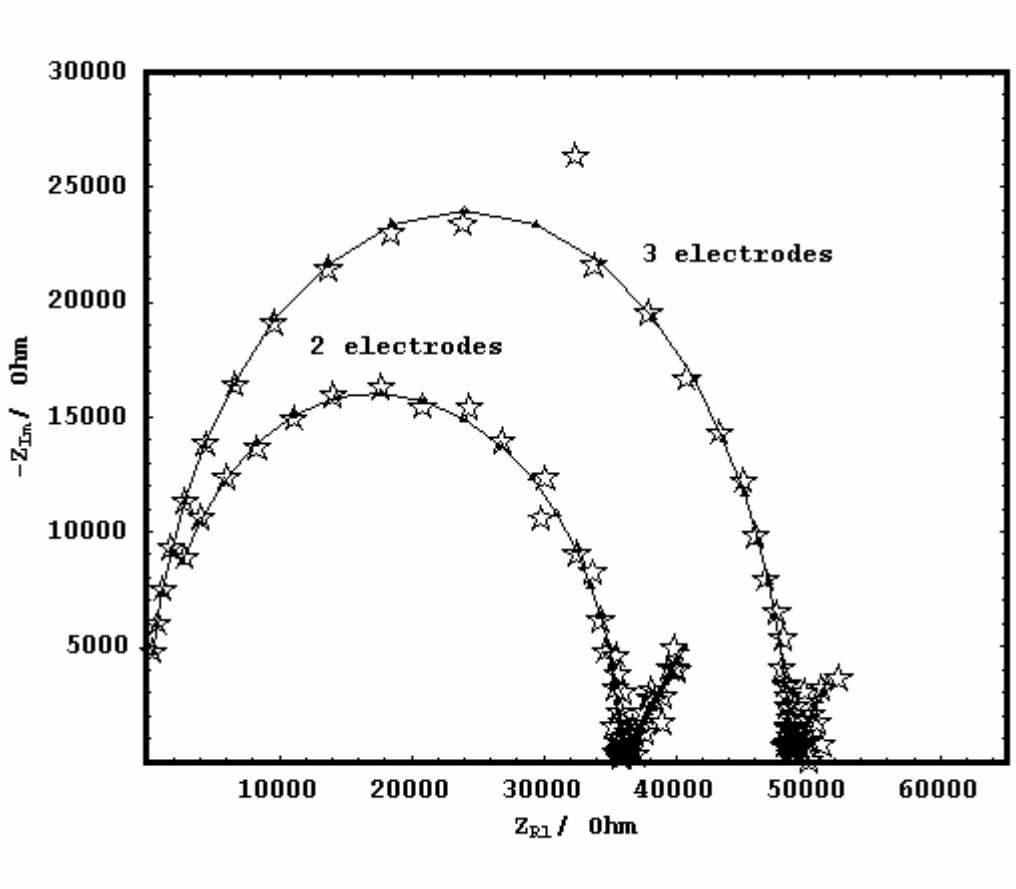

Figure B-2
Comparison of EIS for the Different Electrodes Schemes: AVTSol-1, RDE-2 at 23°C (73°F) (Runs *ard2i* and *ard3i*). The Solid Lines Correspond to the Data Fitting by the Electrochemical Circuit Cell Model.

Comparison of the Three-Electrode and Two-Electrode Schemes of EIS and DC Polarization Measurements Using the RDE-2 System

Table B-1
Corrosion Current, Corrosion Potential, and Charge Transfer Coefficients for Carbon Steel SA210A1 in Aqueous Solution AVTSol-1 (NaCl + NH_4OH: 100 ppb of Cl^- and pH=9) at 23°C (73°F) for the Different Electrode Schemes

Run #	I_{corr} /A	E_{corr} /V	α_1	α_2	Explanations
ard11t	$1.7 \cdot 10^{-6}$	-0.31	0.044	0.053	3 electrodes, 260 RPM
ard12t	$6.2 \cdot 10^{-7}$	-0.50	0.066	0.30	2 electrodes, 260 RPM

Table B-2
Corrosion Charge Transfer Resistance, Double Electric Layer Capacity, and Estimated Corrosion Current for Carbon Steel SA210A1 in Aqueous Solution AVTSol-1 (NaCl + NH_4OH: 100 ppb of Cl^- and pH=9) at 23°C (73°F)

Run #	R_{SOL} / Ohm	R_{CT} / Ohm	C_{DEL} / F	I_{CORR}^{CT} / A	Explanations
ard3i	31000	4700	$2.5 \cdot 10^{-9}$	$2.7 \cdot 10^{-6}$	2 electrodes, 260 RPM

Export Control Restrictions

Access to and use of EPRI Intellectual Property is granted with the specific understanding and requirement that responsibility for ensuring full compliance with all applicable U.S. and foreign export laws and regulations is being undertaken by you and your company. This includes an obligation to ensure that any individual receiving access hereunder who is not a U.S. citizen or permanent U.S. resident is permitted access under applicable U.S. and foreign export laws and regulations. In the event you are uncertain whether you or your company may lawfully obtain access to this EPRI Intellectual Property, you acknowledge that it is your obligation to consult with your company's legal counsel to determine whether this access is lawful. Although EPRI may make available on a case-by-case basis an informal assessment of the applicable U.S. export classification for specific EPRI Intellectual Property, you and your company acknowledge that this assessment is solely for informational purposes and not for reliance purposes. You and your company acknowledge that it is still the obligation of you and your company to make your own assessment of the applicable U.S. export classification and ensure compliance accordingly. You and your company understand and acknowledge your obligations to make a prompt report to EPRI and the appropriate authorities regarding any access to or use of EPRI Intellectual Property hereunder that may be in violation of applicable U.S. or foreign export laws or regulations.

Printed on recycled paper in the United States of America

The Electric Power Research Institute (EPRI)

The Electric Power Research Institute (EPRI), with major locations in Palo Alto, California, and Charlotte, North Carolina, was established in 1973 as an independent, nonprofit center for public interest energy and environmental research. EPRI brings together members, participants, the Institute's scientists and engineers, and other leading experts to work collaboratively on solutions to the challenges of electric power. These solutions span nearly every area of electricity generation, delivery, and use, including health, safety, and environment. EPRI's members represent over 90% of the electricity generated in the United States. International participation represents nearly 15% of EPRI's total research, development, and demonstration program.

Together...Shaping the Future of Electricity

Program:

Boiler and Turbine Steam and Cycle Chemistry

1010187

ELECTRIC POWER RESEARCH INSTITUTE

3420 Hillview Avenue, Palo Alto, California 94304-1395 • PO Box 10412, Palo Alto, California 94303-0813 USA

800.313.3774 • 650.855.2121 • askepri@epri.com • www.epri.com